Contents

A1. Factual information

A1.7 Meteorological information

This annex to the final report discusses the meteorological aspects of the accident in more detail. The key points are referenced in the main report. Some discussions and figures might need specific knowledge for a full understanding. However, where possible, the descriptions are aimed at interested, but not necessarily specialised readers. The references in the footnotes will help readers find further useful information.

For technical terms and abbreviations, please refer to the glossary.

Swiss geographical names can be found via swisstopo[1].

All of the times mentioned in this report, unless otherwise indicated, are given in Central European Summer Time (CEST), i.e. local time (LT) in Switzerland. The relationship between LT, CEST and UTC (Coordinated Universal Time) is: LT = CEST = UTC + 2 h. Even when the primary information was given in UTC, the times in the text and in captions are given in LT.

A1.7.1 General weather conditions

The Alps were within an extension of the Azores anticyclone (high-pressure system). The flat pressure distribution and the vertical temperature profile were supporting the formation of cumulus clouds including isolated TCUs and CBs. The wind at the altitude of the main ridges and above was from the northern sector. The freezing level was between about 4,400 m AMSL in the south of the Alps, and 4,600 m AMSL in the north.

A1.7.2 Weather at the time and location of the accident

The following information about the weather conditions at the time and location of the accident is based on data sources described in sections A1.7.11, A1.7.12, and A1.7.14.3.

In the Alpine region of the accident (cantons of Glarus and Grisons), warm and sunny weather prevailed. The base of the cumulus clouds was around 10,000 ft AMSL (2,800 to 3,400 m AMSL). Above the Segnes pass between the Vorab mountain and Piz Segnas, the wind at the altitude of the flight was blowing from north to north-west. In combination with the thermal activity above the sunny slopes, this created turbulent conditions within the steep side valley (see sections A1.7.7 as well as A1.7.12 to A1.7.15). At the altitude of the flight in this region, the atmosphere was 13 °C warmer than ISA[2], which corresponded to a density altitude of 10,100 ft AMSL (3,080 m AMSL).

Please note that the temperature enhancement against ISA is not a universal constant for all altitudes. For a typical summertime temperature profile with 10 °C/km temperature decrease with altitude, the positive difference to ISA (cooling with only 6.5 °C/km) decreases with altitude. At the time of the departure from Locarno, the temperature was ISA+17 °C in contrast to the ISA+13 °C at about 2,750 m AMSL.

[1] https://map.geo.admin.ch/?topic=swisstopo&lang=en&bgLayer=ch.swisstopo.pixelkarte-farbe

[2] ISA: International Standard Atmosphere according to ICAO, the International Civil Aviation Organization

The archived images from the weather radar network of MeteoSwiss[3] (see section A1.7.10) were showing weak showers about 7 km west of the accident, and 15 to 20 km west of it. The cumulus clouds above Piz Segnas can be seen on the webcam images shown in section A1.7.8.

Weather/clouds	3 to 4 oktas cumulus clouds Base at about 10,000 ft AMSL (3,000 m AMSL)
Visibility	More than 10 km
Wind	Crap Masegn station[4], 009° / 16 kt, 26 kt in gusts COSMO analysis[5] at the altitude of flight 340° / 18 kt (± gusts) Station 4 km south[6], 10 kt from north, with gusts in the vicinity of the accident[7] 060-070° / 17 kt
Temperature / dew point	Crap Masegn station, 14.9 °C / 6.7 °C COSMO analysis at the flight's altitude, 10.5 °C / 7.4 °C
Atmospheric pressure	Crap Masegn station, 762.3 hPa (QNH 1,030.8 hPa) COSMO analysis at 2,750 m AMSL, 738.3 hPa QNH south of the Alps (LSZL), 1,014 hPa QNH north of the Alps (LSMD), 1,017 hPa (QNH: pressure reduced to sea level, as calculated according to ICAO[8])
Hazards[9]	*"Isolated showers and thunderstorms, especially over the mountains. Temperature exceeding 30-degree centigrade (consider the density altitude)."*

A1.7.3 Astronomical information

Position of the sun[10]	Azimuth: 252°	Elevation: 39°
Light conditions	Daytime	

[3] MeteoSwiss is the short name for the Federal Office of Meteorology and Climatology: https://www.meteoswiss.admin.ch/home.html?tab=overview

[4] Meteorological station of MeteoSwiss at 2,480 m AMSL next to the site of the accident (wind at 2,495 m AMSL; temperature and pressure at 2,482 m AMSL; see sections A1.7.11.2 and A1.7.14.3)

[5] Fine-mesh meteorological model of MeteoSwiss (see section A1.7.12)

[6] Meteorological station of Flims Electric AG (see section A1.7.14.3)

[7] Derived from the moving dust cloud after the impact, documented in a video

[8] ICAO, the International Civil Aviation Organization, defining the ISA, the International Standard Atmosphere

[9] Translated from the aviation weather forecast of MeteoSwiss from 13:00 LT (see section A1.7.5.1)

[10] https://www.esrl.noaa.gov/gmd/grad/solcalc/

A1.7.4 Airport weather reports

The following sections contain many abbreviations and codes, which are explained in the glossary. For French or Italian explanations, see the brochure[11].

These reports (Meteorological Aviation Routine Weather Report – METAR) have no direct relevance to the accident. However, the reports that were valid well before departure until the planned landing are listed here. They are referenced in section A1.7.16.1).

Between 14:20 LT and 18:50 LT, the following reports were issued (the times in the messages are in UTC, i.e. 041220Z is denoting the fourth day of the month at 14:20 LT):

[11] https://www.meteosuisse.admin.ch/content/dam/meteoswiss/fr/service-und-publikationen/publikationen/doc/MCH_Flugwetter_2020_F_Web.pdf and https://www.meteosvizzera.admin.ch/content/dam/meteoswiss/it/service-und-publikationen/doc/MCH_Flugwetter_2020_I_Web.pdf

METAR from Locarno Aerodrome (LSZL)

041220Z AUTO 27006KT 9999NDV NCD 30/21 Q1015 RMK=
041250Z AUTO 25006KT 230V290 9999NDV NCD 30/21 Q1015 RMK=
041320Z AUTO 26006KT 220V300 9999NDV NCD 31/22 Q1015 RMK=
041350Z AUTO 26005KT 9999NDV NCD 31/22 Q1014 RMK=
041420Z AUTO 26005KT 9999NDV NCD 31/22 Q1014 RMK=
041450Z AUTO 27004KT 230V300 9999NDV NCD 32/21 Q1014 RMK=
041520Z AUTO 27005KT 230V290 9999NDV NCD 32/21 Q1014 RMK=
041550Z AUTO 28005KT 230V330 9999NDV FEW160 32/21 Q1013 RMK=
041650Z AUTO 28003KT 230V340 9999NDV NCD 31/21 Q1014 RMK=

METAR from Lugano Airport (LSZA):

041220Z 20008KT 9999 FEW060 32/20 Q1016 NOSIG=
041250Z 19007KT 9999 FEW060 32/20 Q1016 NOSIG=
041320Z 20007KT 9999 FEW060 33/20 Q1016 NOSIG=
041350Z 20007KT 9999 FEW060 33/19 Q1015 NOSIG=
041420Z 20007KT 9999 FEW060 33/19 Q1015 NOSIG=
041450Z 19006KT 9999 FEW060 33/19 Q1015 NOSIG=
041520Z AUTO 19007KT 9999 //////TCU 33/20 Q1014=
041550Z 19008KT 9999 SCT060 32/20 Q1014 NOSIG=
041620Z 19008KT 9999 FEW060 32/20 Q1015 NOSIG=
041650Z 19006KT 150V220 9999 FEW060 32/20 Q1015 NOSIG=

METAR from Dübendorf Air Base (LSMD):

041220Z AUTO VRB03KT 9999NDV NCD 33/14 Q1018 RMK=
041250Z AUTO VRB05KT 9999NDV FEW083 33/14 Q1018 RMK=
041320Z AUTO 16004KT 120V240 9999NDV SCT082 33/14 Q1018 RMK=
041350Z AUTO 35006G18KT 290V060 9999NDV BKN081 BKN100 32/15 Q1018 RMK=
041420Z AUTO VRB05KT 9999NDV FEW078 SCT098 33/15 Q1017 RMK=
041450Z AUTO 03005KT 300V080 9999NDV FEW079 33/17 Q1017 RMK=
041520Z AUTO 03005KT 330V100 9999NDV NCD 33/15 Q1017 RMK=
041550Z AUTO 01005KT 320V060 9999NDV NCD 33/13 Q1017 RMK=
041650Z AUTO 02004KT 330V120 9999NDV NCD 32/15 Q1018 RMK=

METAR from Zurich Airport (LSZH)

041220Z 03005KT 270V090 9999 SCT065 FEW070TCU 35/14 Q1018 NOSIG=
041250Z 32014KT 9999 SCT065 FEW070TCU 33/16 Q1018 NOSIG=
041320Z 35009KT 9999 SCT060 FEW068TCU 34/16 Q1018 NOSIG=
041350Z 36008KT 320V030 9999 FEW068 FEW070TCU SCT120 34/16 Q1018 NOSIG=
041420Z 36008KT 320V040 9999 FEW070 FEW075CB 33/17 Q1018 NOSIG=
041450Z 36006KT 330V040 9999 FEW075TCU SCT130 33/16 Q1017 NOSIG=
041520Z 02009KT 320V060 9999 FEW075TCU SCT130 34/15 Q1017 NOSIG=
041550Z 36005KT 330V030 9999 FEW075TCU SCT140 33/13 Q1017 NOSIG=
041620Z 36005KT 320V040 9999 FEW075TCU SCT140 33/15 Q1017 NOSIG=
041650Z 36005KT 240V030 9999 FEW075TCU BKN200 31/16 Q1018 NOSIG=

A1.7.5 Forecasts

A1.7.5.1 General aviation weather forecast text from MeteoSwiss

At 07:00 and 13:00 LT, texts for the general aviation forecasts in Switzerland were issued in German and French.

The complete German texts are copied in the German version of this annex. Here, the French texts are copied. Only the core statements, which are underlined, are translated in a summary after the forecasts.

"Prévision aéronautique pour la Suisse, valable du samedi 4 août, au mardi 7 août 2018. Bulletin de 5h00 UTC

Situation générale :

léger affaissement de la dorsale en altitude mais toujours anticyclonique en surface.

Temps, nuages et visibilité entre 6 et 12 UTC :

Plateau et Jura : plutôt clair au début, hormis quelques nuages élevés. Développement à la mi-journée de 1-3/8, bases 7000-9000 ft/msl suivi d'averses isolées, voire orages. Visibilité supérieure à 8 km.

Préalpes et Alpes : encore parfois 3-4/8 de nuages résiduels au début dans les Alpes orientales, bases vers 10000 ft/msl, se dissipant rapidement, sinon clair. Développement à la mi-journée de 1-3/8, bases 7000-9000 ft/msl suivi d'averses isolées, voire orages. Visibilité supérieure à 8 km.

Sud des Alpes et Engadine : encore 3-5/8 de nuages résiduels au début en Engadine, bases vers 10000 ft/msl, se dissipant rapidement, sinon clair. Développement à la mi-journée de 1-3/8, bases 4500-6000 ft/msl au Sud, 7000-9000 ft/msl le long du massif alpin, 9000-11000 ft/msl en Engadine. Visibilité généralement supérieure à 8 km.

Dangers prévus entre 6 et 12 UTC :

Température supérieure à 30°C, altitude-densité élevée.

Evolution jusqu'à minuit, dangers compris :

Averses ou orages isolés au Nord cet après-midi et début de soirée. Dissipation en soirée. Augmentation du risque d'orage en soirée au Sud des Alpes.

Vent (en degrés et kt) et températures :

	Payerne		Zürich		Lugano	
	9 UTC	15 UTC	9 UTC	15 UTC	9 UTC	15 UTC
Au sol	NE / 2-5 KT		VRB / 1-4 KT		VRB / 1-4 KT	
05000 FT	055/010 PS20	055/010 PS22	020/005 PS19	060/005 PS22	150/005 PS18	230/010 PS22
10000 FT	040/015 PS07	020/010 PS09	030/010 PS06	335/010 PS08	025/010 PS08	015/015 PS10
18000 FT	350/015 MS05	320/015 MS06	355/015 MS05	335/015 MS06	030/015 MS05	025/015 MS05
30000 FT	290/010 MS33	295/015 MS33	275/010 MS33	280/020 MS33	040/020 MS33	315/005 MS32
39000 FT	290/015 MS55	265/020 MS55	280/010 MS55	265/025 MS55	020/010 MS54	315/010 MS54
53000 FT	335/010 MS60	280/005 MS60	330/010 MS60	270/005 MS59	005/005 MS60	350/005 MS60
Vent max	-----FT ---/---					
Tropopause	41000FT MS58					
Isotherme zéro	15000FT					

Tendance pour les trois prochains jours : […]

Prochaine actualisation : samedi, 4 août 2018, à 11h00 UTC=

Prévision aéronautique pour la Suisse, valable du samedi 4 août, au mardi 7 août 2018. Bulletin de 11h00 UTC.

Situation générale :

léger affaissement de la dorsale en altitude mais toujours anticyclonique en surface.

Temps, nuages et visibilité entre 12 et 18 UTC :

Plateau et Jura : 3-5/8, bases 7000-9000 ft/msl. Visibilité généralement supérieure à 8 km. Averses ou orages isolés sur le Jura avec abaissement temporaire du plafond et une réduction de la visibilité.

Préalpes et Alpes : 3-5/8, bases 8000-10000 ft/msl. Visibilité généralement supérieure à 8 km. Averses ou orages isolés sur les Préalpes avec abaissement temporaire du plafond et une réduction de la visibilité.

Sud des Alpes et Engadine : 3-5/8, bases 7000-9000 ft/msl, 9000-11000 en Engadine. Visibilité généralement supérieure à 8 km. Averses ou orages isolés sur les versants sud-alpins avec abaissement temporaire du plafond et une réduction de la visibilité.

Dangers prévus entre 12 et 18 UTC :

Averses ou orages isolés sur les reliefs. Température supérieure à 30°C, altitude-densité élevée.

Evolution jusqu'à minuit, dangers compris :

A nouveau clair par le nord-ouest, dernières averses ou orages isolés au Sud.

Vent (en degrés et kt) et températures au sol et en altitude :

	Payerne		Zürich		Lugano	
	12 UTC	18 UTC	12 UTC	18 UTC	12 UTC	18 UTC
Au sol	NE/ 5-10		N/NE 5-10		VRB/2-7	
05000 FT	045/010 PS21	050/020 PS22	285/005 PS21	025/015 PS21	235/010 PS20	245/005 PS22
10000 FT	040/020 PS08	030/010 PS09	005/020 PS07	340/010 PS08	025/015 PS09	020/015 PS09
18000 FT	355/010 MS06	335/010 MS06	340/010 MS06	320/015 MS06	005/010 MS05	020/010 MS06
30000 FT	270/015 MS32	300/015 MS33	275/020 MS33	290/015 MS33	025/010 MS32	295/010 MS32
39000 FT	270/015 MS54	255/020 MS55	265/015 MS54	260/020 MS55	040/005 MS54	290/010 MS54
53000 FT	005/005 MS60	295/015 MS60	325/005 MS60	305/010 MS59	015/005 MS61	315/005 MS60
Vent max	-----FT ---/---					
Tropopause	42000FT MS60					
Isotherme zéro	14300FT					

Tendance pour les trois prochains jours : […]"

End of the excerpts from the French version of the general aviation forecast.

Summary: In the two forecasts (the first valid for 08:00 to 14:00 LT, the second for 14:00 to 20:00 LT), the development of clouds over the Alpine region was described with initially 1 to 3 oktas, followed by 3 to 5 oktas with cloud bases between 7,000 and 9,000 ft AMSL, and 8,000 to 10,000 ft AMSL, respectively. For both periods, the visibility was estimated to be more than 8 km. The possibility for isolated thunderstorms was mentioned in the general texts, and in the warnings for the afternoon's forecast. In both warnings, the elevated density altitude was mentioned. The wind at 10,000 ft AMSL above Zurich and Lugano (as shown in the tables) was expected from the northern sector with 10 to 15 kt during the afternoon (no indication for above the Alps).

A1.7.5.2 Significant weather chart for the Alps

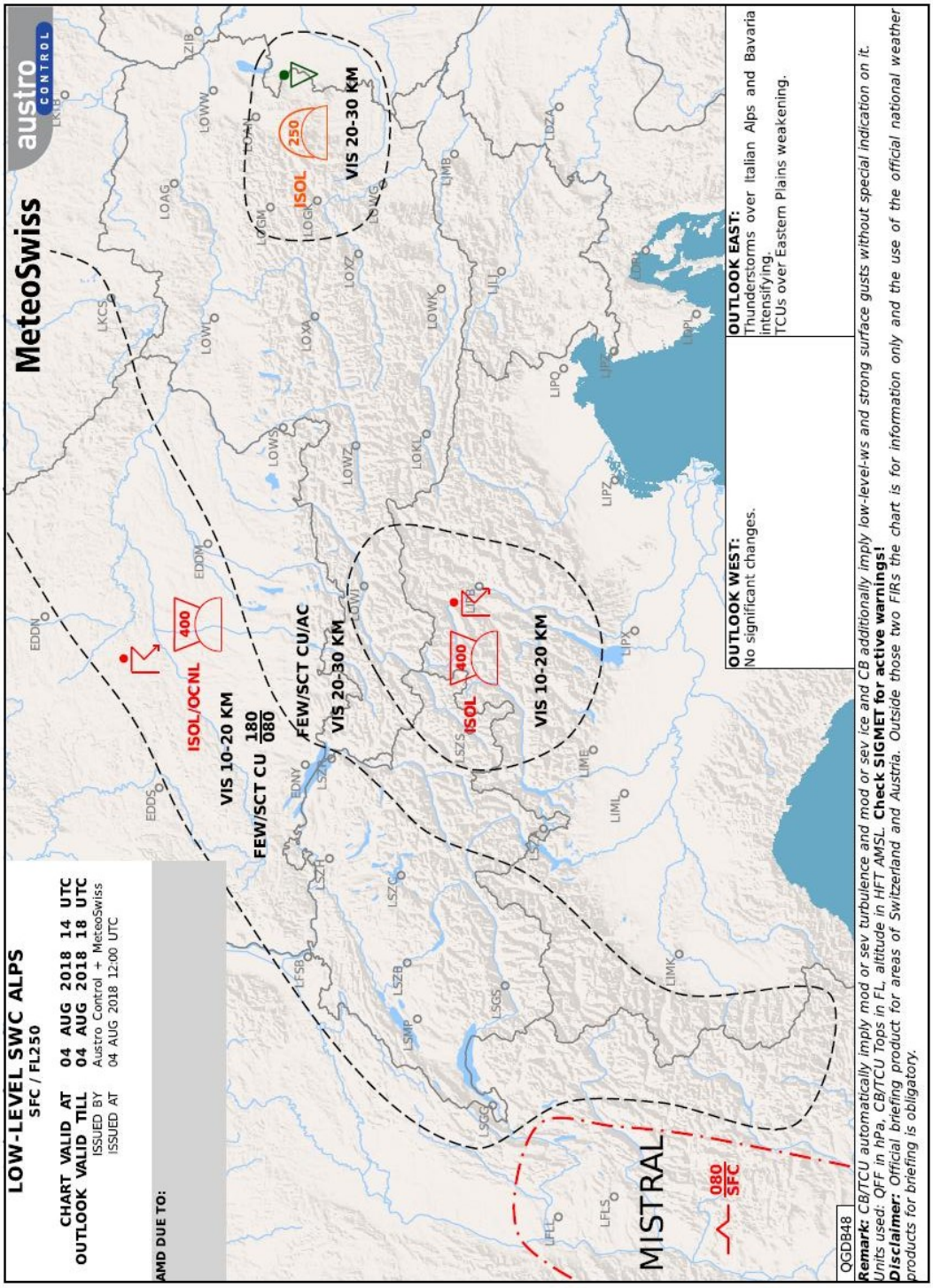

Figure 1: This LOW-LEVEL SWC ALPS was issued at 14:00 LT and was valid for 16:00 to 20:00 LT. The symbols are explained in the document from MeteoSwiss[12]. For south-western Switzerland, isolated showers and thunderstorms are shown with good visibility. Similarly, but only occasionally, this was indicated for the western region which included the destination airfield Dübendorf (south of LSZH).

[12] There is no English version available. However, this link is for a French description: https://www.mete-osuisse.admin.ch/content/dam/meteoswiss/fr/service-und-publikationen/beratung-und-service/doc/Prospekt_Low-Level-SWC_F_v5.pdf

A1.7.5.3 General aviation forecast for the main VFR routes

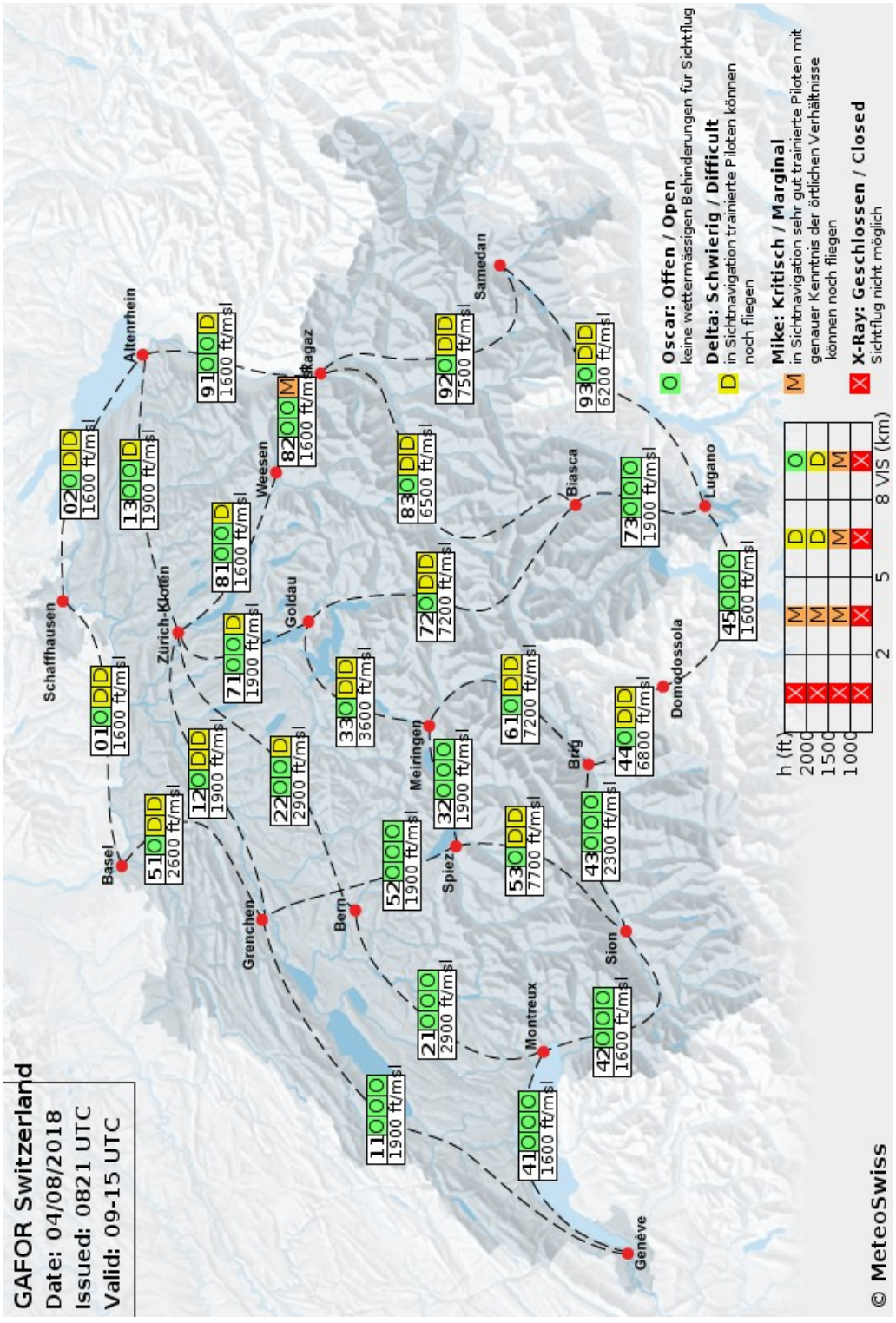

Figure 2a: The GAFOR charts for 11:00 to 17:00 LT (this page) and for 14:00 to 20:00 LT (next page) are not showing any closed routes. With the second GAFOR of the day (next page), there were also no marginal routes left. The route crossing the Segnes pass is between the routes no. 72 and 83. Each character in the boxes denotes two hours within the six-hour periods of the two GAFOR charts. The elevations indicated as 'ft/msl' are reference altitudes in ft AMSL for those routes (e.g. elevations of passes). The classifications O/D/M/X are explained on the bottom right of the chart. Continued in figure 2b.

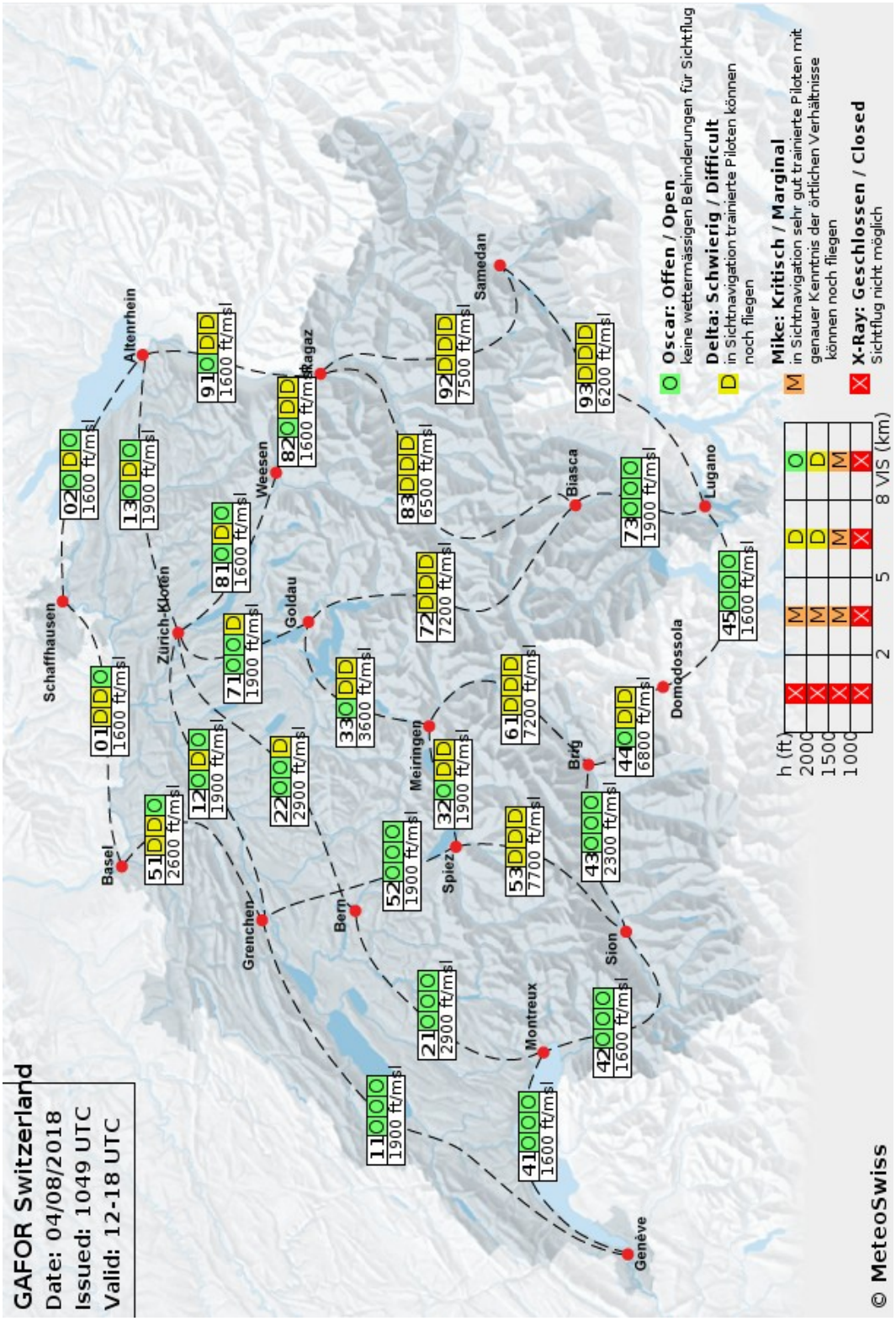

Figure 2b: Continued from 2a. More explanations about the codes can be found in the document of MeteoSwiss (see footnote 11 on page 4). Despite the good visibility, some routes (including 72 and 83) are classed as 'difficult', probably due to the possibility of isolated TCUs and CBs. Wind is not factored into these GAFOR charts. Source: Federal Office of Meteorology and Climatology.

A1.7.5.4 Terminal aerodrome forecast

During the hours before and after the accident (until after the planned landing time), the following terminal aerodrome forecasts (TAFs) were issued (times in UTC, i.e. the header 040825Z 0409/0418 is declaring that the forecast was published at 10:25 LT, valid for 11:00 to 20:00 LT on this day):

TAF SHORT for Lugano Airport (LSZA)
(for Locarno, no TAF is issued on weekends)

```
040825Z 0409/0418 VRB03KT CAVOK=

041125Z 0412/0421 20007KT 9999 FEW060TCU=

041425Z 0415/0424 20007KT 9999 FEW060 PROB40 TEMPO 0415/0424 SHRA
SCT060TCU PROB40 TEMPO 0418/0423 01015G27KT 4000 TSRA SCT050CB=
```

TAF LONG for the Dübendorf Airbase (LSMD)

```
040925Z 0410/0516 VRB03KT CAVOK TEMPO 0410/0420 9999 FEW070
PROB30 TEMPO 0412/0419 TSRA FEW050CB=
```

TAF LONG for Zurich Airport (LSZH)

```
040825Z 0409/0515 VRB03KT CAVOK TX34/0415Z TN17/0504Z TX34/0515Z
BECMG 0409/0412 9999 FEW050 PROB30 TEMPO 0412/0415 35010KT
FEW050TCU TEMPO 0414/0420 04007KT BECMG 0417/0420 CAVOK
BECMG 0510/0513 04008KT 9999 FEW050=

041125Z 0412/0518 VRB03KT 9999 FEW065 TX34/0415Z TN17/0504Z
TX34/0515Z PROB40 TEMPO 0412/0414 31013G25KT FEW060CB TEMPO
0414/0421 04007KT BECMG 0417/0420 CAVOK BECMG 0510/0513 04008KT
9999 FEW050=

041425Z 0415/0521 36008KT 9999 FEW068 FEW070TCU TX35/0415Z
TN17/0504Z TX34/0515Z PROB30 TEMPO 0415/0417 FEW065CB TEMPO
0416/0421 04006KT BECMG 0417/0420 CAVOK BECMG 0509/0512 9999
FEW050 TEMPO 0513/0521 04008KT PROB30 TEMPO 0512/0516 4000 TSRA
SCT050CB=
```

A1.7.6 Warnings

No AIRMET or SIGMET was issued for the time and the airspace of this flight. However, in the text for the general aviation forecast (see section A1.7.5), the elevated density altitude and the possibility for thunderstorms was mentioned.

A1.7.7 Weather descriptions by eyewitnesses

The pilot of the first rescue helicopter at the scene of the accident has described the wind situation 15 minutes after the accident at 17:10 LT. He encountered strong winds from the north-east when passing the Segnes pass and on its south side. He mentioned that the wind there was not laminar, and that south of the Martinsloch, the helicopter was hit by a gust. The pilot decided on an approach from the south-west into the wind. He pointed out that, during the flat approach, the wind became laminar at about 20 kt, and he felt the laminar mountain wind when leaving the helicopter.

The ambulance officer added that he could only use his mobile phone when protecting it with his jacket against the wind, which was blowing from the direction of Piz Segnas.

The pilot of the second rescue helicopter reported similar observations. The crew was guided for an approach from south to north and was informed about a strong

wind from the north. The pilot estimated the base of 3 to 5 oktas TCUs at an altitude of about 9,000 to 10,000 ft AMSL and observed considerable horizontal and vertical movement within the clouds. The visibility was described as 'unlimited' outside of the clouds. During the approach, it seemed to the pilot that a thunderstorm might be imminent. However, this did not transpire and the clouds began to dissipate with lowering sun elevation. The wind at the location of the accident was described to be strong and laminar, with an estimated speed of 20 to 25 kt from the north, and from a north-eastern direction above the mountains. The pilot expected turbulence at the landing site behind the crests surrounding the small basin near Las Palas and Piz Segnas.

The instructor of a single-engine aircraft (Cessna 152), who crossed the Segnes pass with his student shortly before the Ju 52 aeroplane, described their impressions and decisions. They encountered extended downdraughts in the Flims region. He mentioned that it was difficult to maintain the planned altitude of about 9,100 ft AMSL (2,800 m AMSL). The instructor remembered a discussion with his student about the best way to enter the basin in front of the pass while always having an option for a safe return even if the downdraughts persisted. He reported that the Cessna was lifted again on their track along the western slope of the Swiss mountain called Atlas. He continued that shortly before crossing the pass, another downdraught interrupted the updraughts, before the ridge could be crossed at a safe height. The question as to whether extraordinary turbulence was encountered was answered negatively. The instructor added that clouds were not a problem throughout the day.

An image of the Cessna, captured shortly before crossing the Segnes pass, can be found in the main report (see figure 10).

The following description is an example from the public's response – in this case, from an experienced glider pilot with a professional background in meteorology. He mentioned that the Flimserstein high plateau and the ridge between Crap Sogn Gion and Crap Masegn is well known among glider enthusiasts in the Alps as one of the strongest and most reliable sources for thermals. In between, distinct and extended downdraught regions are well known, especially when there is a tendency for north-easterly winds aloft. He mentioned a personal experience about two weeks before the accident where he happily flew at 3,000 m AMSL near Flimserstein, expecting to cross the Segnes pass without any problems. However, he was washed down at between 5 and 8 km from the crest and was forced to change his route. He thought that the large-scale sinking on the downwind side was caused by forced lifting on the cooler northern side of the ridge. Within this widely sinking flow, only the strongest local thermals could persist.

Local people and our staff who worked near the two meteorological stations during the summer of 2019 (see section A1.7.14) confirmed that a robust downslope wind along the basin and the Segnas Sut high plateau typically developed during afternoons. The continuous meteorological measurements near a water catchment of Flims Electric AG on an elevation of 2,100 m AMSL provide objective evidence for this diurnal wind system (see section A1.7.14.3).

According to an experienced eyewitness on the Segnes pass, the wind speed was at least 60 km/h at the time of the accident. This account is supported by the above-mentioned observations and the fine-scale modelling (see section A1.7.15).

Selected images of clouds received from members of the public are copied in the main report and in other annexes (see e.g. annex A1.1). In the remaining collection, no relevant additional information supplementing the selected pictures and the webcam images has been found.

A1.7.8 Webcams

Figure 3: Three frames of the webcam on Mutta Rodunda[13] (see map in figure 4) viewing towards the north 17 minutes before the accident (16:40 LT, top frame) until three minutes after (17:00 LT, bottom frame). The orange pointer is marking the site of the accident, where the wreckage is faintly visible on the original image. The Segnes pass is marked by the red pointer. Left of the centre of the image is Piz Segnas with Atlas in front. On the right is the Trinserhorn (Piz Dolf) mountain (see map below).

[13] https://laax.roundshot.com/mutta-rodunda/ (for archive, see calendar icon on the right-hand navigation bar)

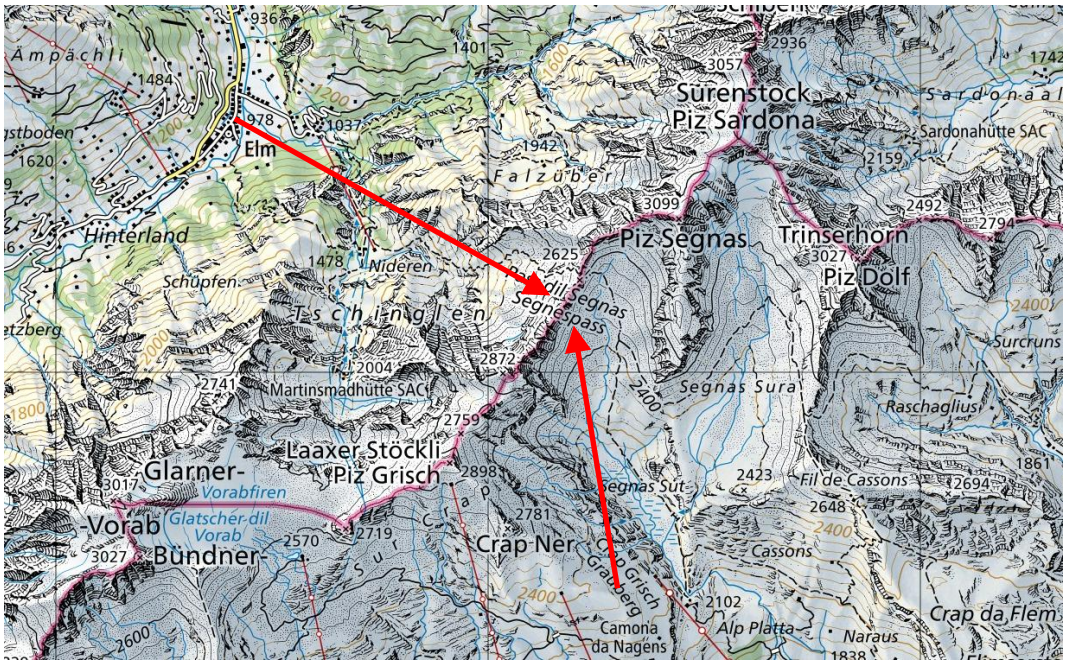

Figure 4: Positions and viewing directions towards the Segnes pass from the two webcams at Mutta Rodunda in the south (figure 3) and in Elm in the north-west (figure 5). Source of the map: Federal Office of Topography.

Figure 5: Two frames from the webcam in Elm around 16:00 LT (top frame) and at about 17:00 LT (bottom). The Segnes pass is within the ridge in the background, almost hidden by the mountain in front of it (solid red pointer). The prominent mountain peak just right of the centre of the images is the Grosses Tschingelhorn. The Martinsloch (dotted pointer) is visible on the webcam when the light is favourable. The site of the accident is behind the ridge between the Martinsloch and the Segnes pass. Based on the hourly imagery of this webcam, it can be concluded that the route from the Segnes pass to Elm was free of clouds during the afternoon, at least at the times of the images.

07:00 LT:

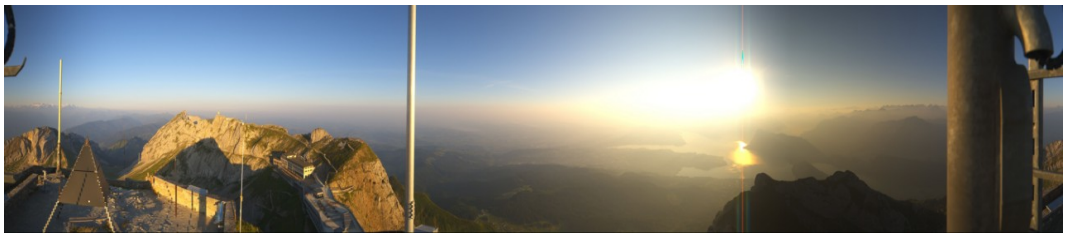

09:00 LT:

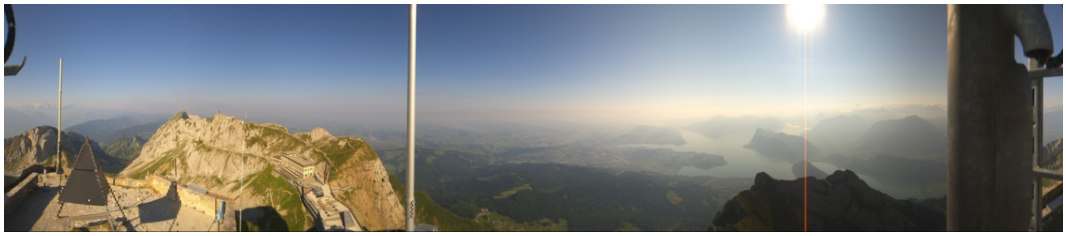

12:00 LT:

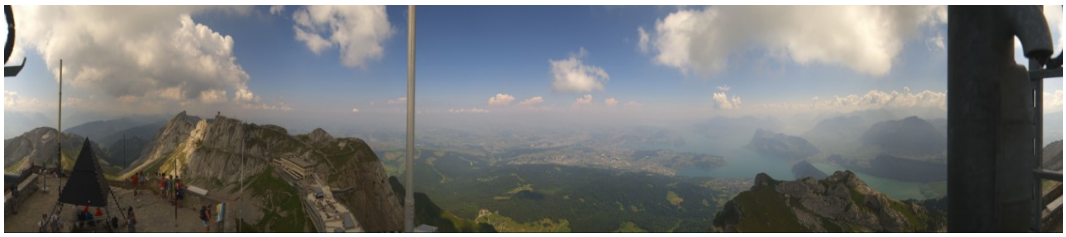

15:00 LT:

16:00 LT:

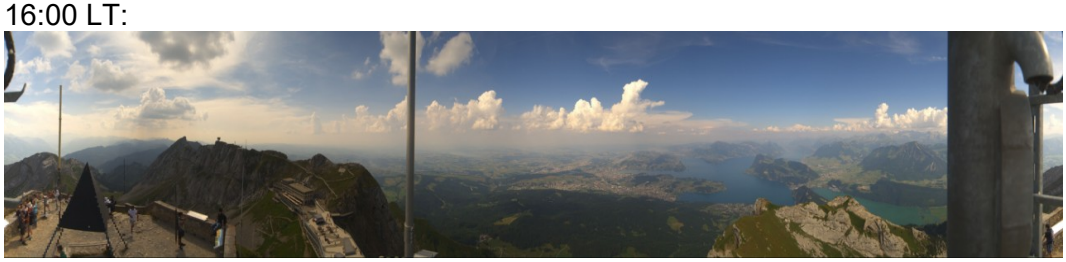

17:00 LT:

Figure 6: Roundshot webcam on Mount Pilatus[14] on 4 August 2018 between 07:00 and 17:00 LT. The images show the cloud development during the day in the wider Alpine area. The thin pole left of the centre roughly marks the north, whereas the south is behind the thick pole, i.e. the southern sector is split between the two edges of the images.

[14] https://pilatus.roundshot.com/ (for archive, see calendar icon on the right-hand navigation bar)

Disentis, viewing from left to right from NE via SE to west at 17:00 LT:

Brugnasco near Airolo, viewing to ENE (left), south and NW (right) at 16:30 LT:

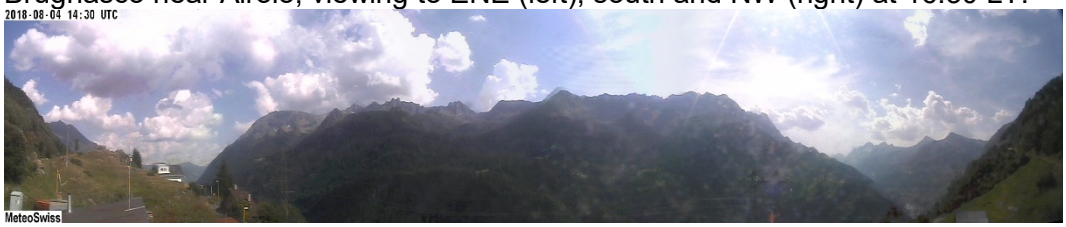

Olivone, viewing towards the west to Punta di Larescia at 16:30 LT:

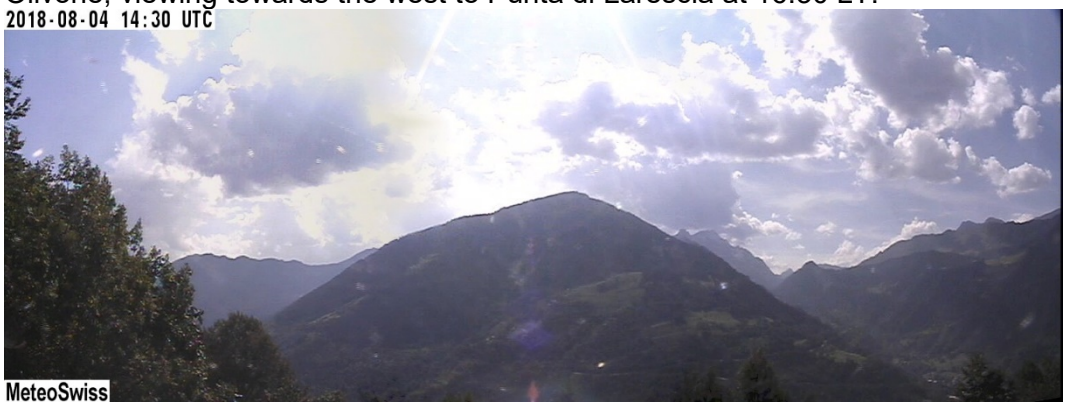

San Salvatore, viewing NNE (left) over Lugano (below centre) at 16:30 LT:

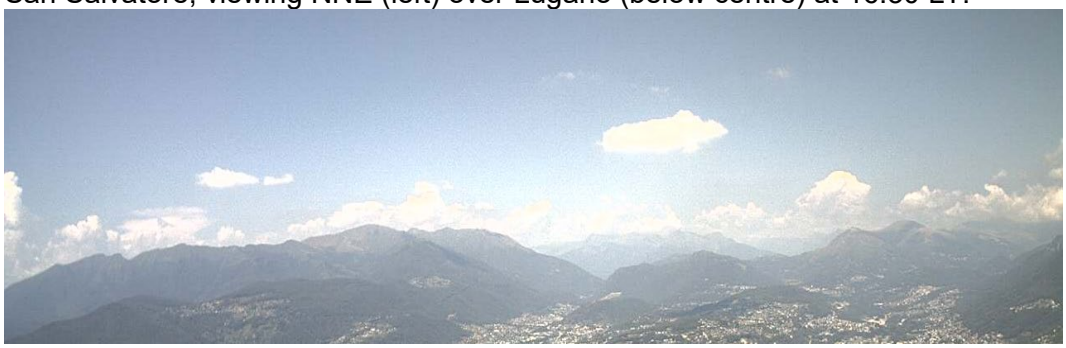

Montagnola, viewing to SW (left) via north to SE (right) at 16:30 LT:

Figure 7: Webcams on the south side of the Alps at 16:30 LT, and from Disentis in the Rhine Valley at 17:00 LT. This large collection of images is archived every 10 minutes by the Federal Office of Meteorology and Climatology.

A1.7.9 Satellite imagery

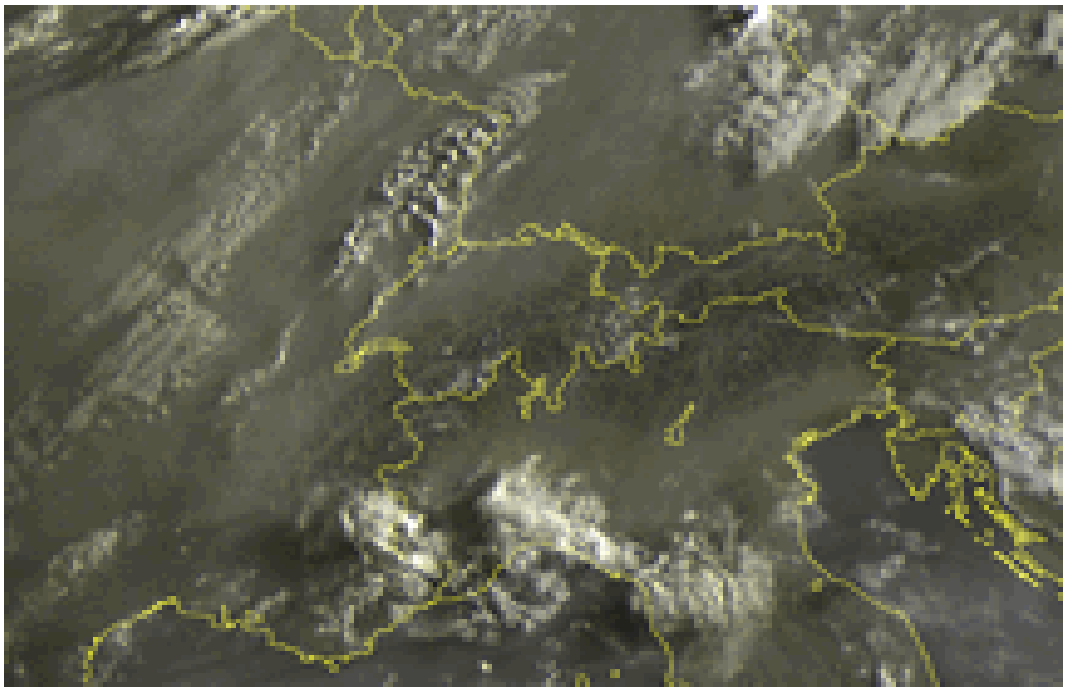

Figure 8: The (visible) satellite image from the geostationary satellite operated by EUMETSAT[15] shows haze over the Swiss Plateau (between Lake Geneva and Lake Constance). No clouds are visible over the Alps.

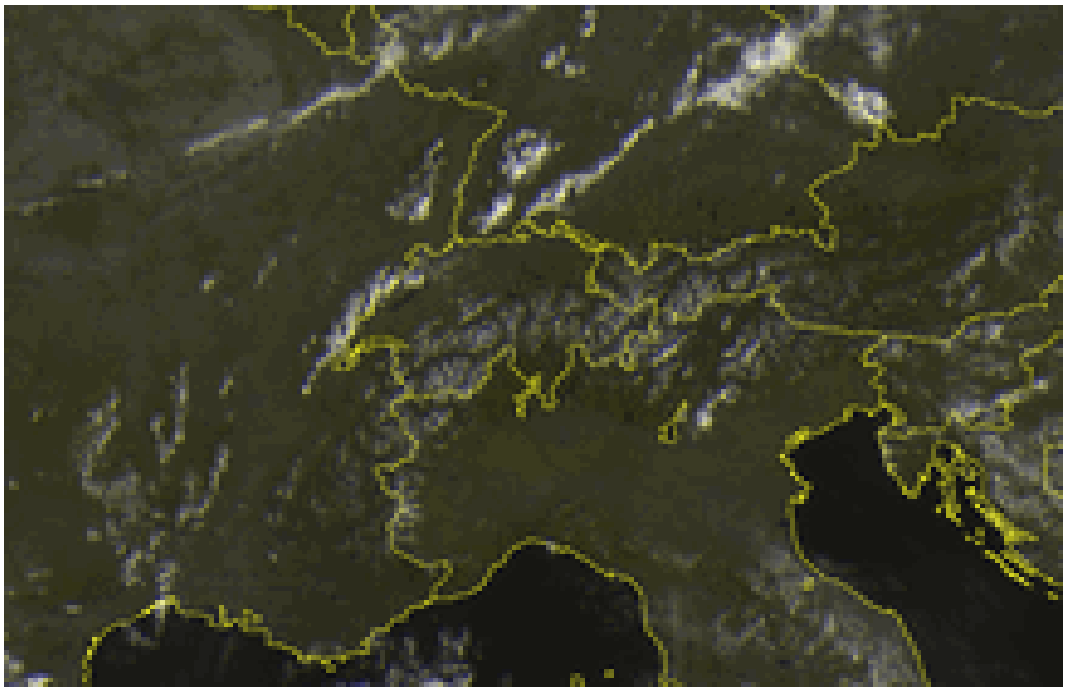

Figure 9: A first convective activity with cumulus clouds over the Jura mountains and north of Switzerland over the Vosges mountains, the Black Forest and the Swabian Alps is visible at 12:00 LT. The small cumulus clouds over the Alps (see figure 6) are not yet discernible due to this coarse resolution.

[15] https://www.eumetsat.int; Source for the satellite images: http://www2.sat24.com/history.aspx?culture=de

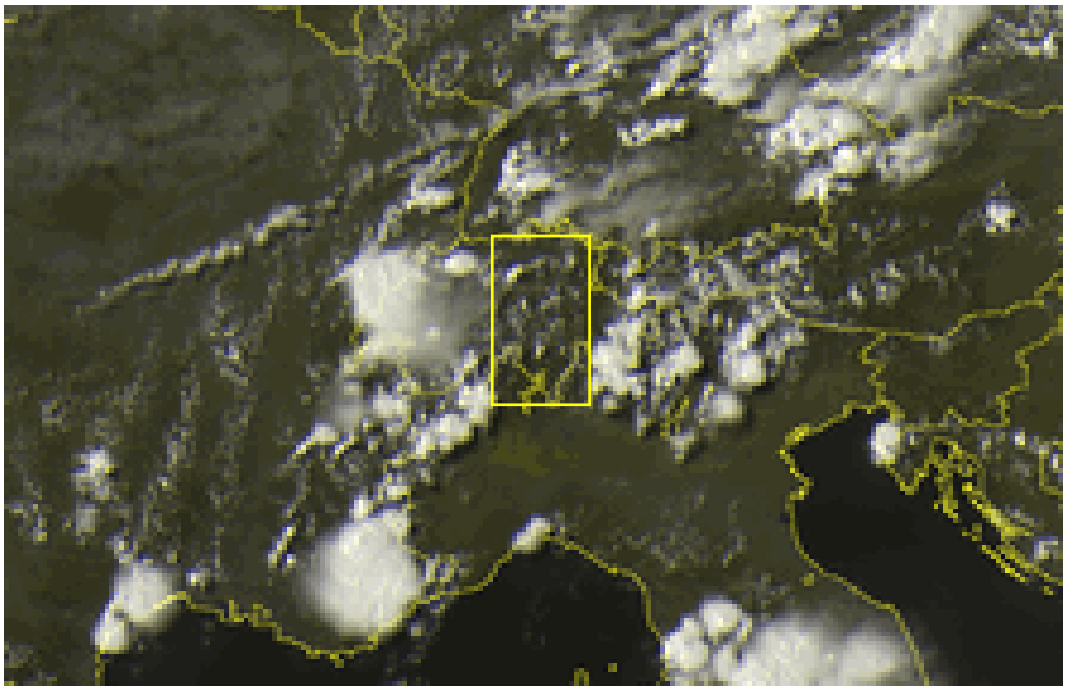

Figure 10: At 17:00 LT, convective areas with CBs had developed west and south-east of the region of interest (yellow rectangle between Ticino and northern Switzerland). Within this zone, around the planned flight, only a few CUs and possible TCUs, but no CBs are visible at the time of the accident.

The corresponding satellite images were screened for the day before, when HB-HOT was flown from Dübendorf in the north to Ticino in the south. This comparison shows a similar beginning to the day, with less convection in the afternoon. For both days, the infrared images showing cloud top altitudes were inspected. They confirm the finding from above in figure 10: there were no CBs in the vicinity of the planned flight.

Higher-resolution images from the lower orbiting Aqua and Terra[16] satellites were screened as well. However, due to their orbital schedule, their imagery was only available between 11:58 LT and 13:42 LT and is therefore not shown here.

A1.7.10 Weather radar imagery

The national weather service operates five weather radar stations that generate an almost complete composite image of the precipitation over Switzerland[17]. The process of generating these well-known images, based on the raw radar echoes, is quite complex. It is a challenge, especially within the Alps, to separate relevant signals (precipitation) from artefacts (e.g. ground clutter). During this process, weak local precipitation signals can sometimes be filtered out. Below the mountain ridges, precipitation can also be hidden. And, in any case, clouds without precipitation are not visible on radar imagery. For volumes in the atmosphere that can be seen from two or more radar stations, the signals can be combined. Please visit the link in the footnote for more details.

The radar station next to the region of interest is located on the Weissfluhjoch summit, about 45 km east of Piz Segnas. It offers a direct view into the Rhine Valley. Therefore, the reliability for the detection of showers was high.

[16] https://worldview.earthdata.nasa.gov/

[17] https://www.meteoswiss.admin.ch/home/measurement-and-forecasting-systems/atmosphere/weather-radar-network.html

Rain from cumulus clouds (CUs, TCUs and CBs) can only come from the formation of ice particles in the cloud. This means that precipitation in the cloud extends up to an altitude well above the freezing level (typically to above - 10 °C). Hence rainfall at the valley floor will be seen even in the case of radar obscuration because the radar will detect the formation of the precipitation above. Therefore, the radar imagery presented here is expected to show a complete picture of precipitation in the area of the accident.

The radar images were generated and archived every two to three minutes, i.e. the temporal resolution is quite high. First echoes on the day and in the region of the accident were visible between 12:40 LT and 13:00 LT near Ilanz. Figure 11 shows the peak activity of this weak shower with only 2 mm/h.

On the webcam, this weak precipitation is not directly visible. Only dark clouds over Ilanz are an indication. Therefore, the webcam image of this weak first shower is not included here.

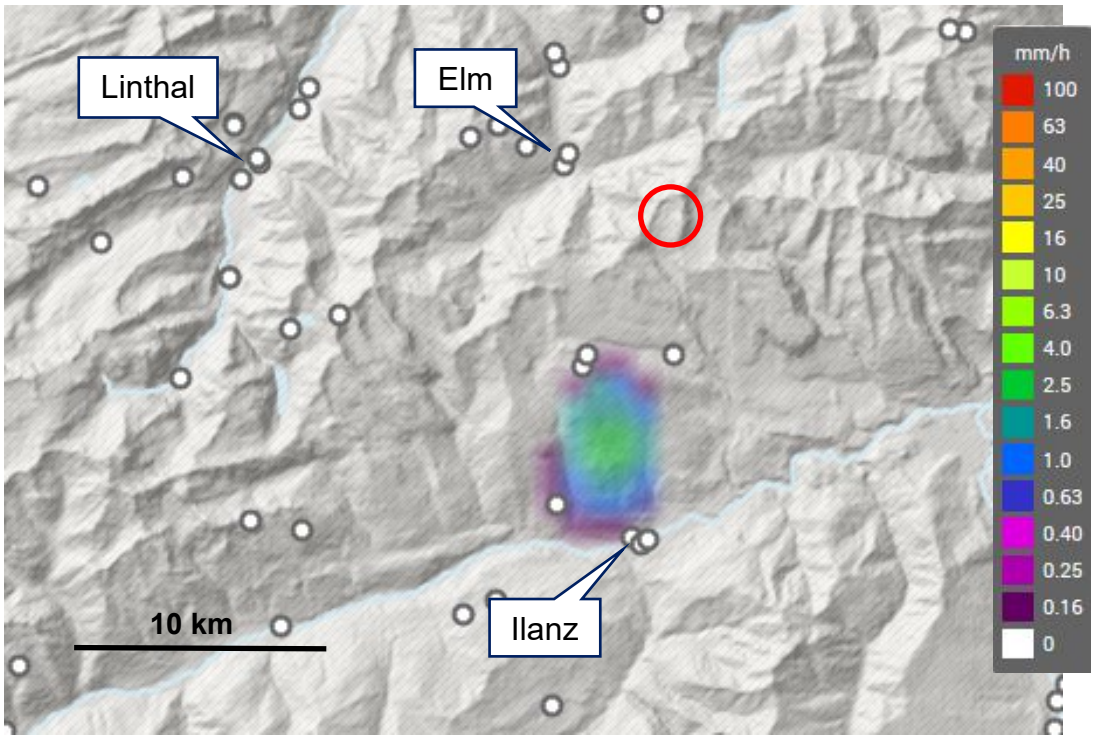

Figure 11: Precipitation radar image at 12:50 LT. The accident happened within the red circle. The small white circles mark the location of surface weather stations. See text below for more information. Source: Federal Office of Meteorology and Climatology, MeteoSwiss, via GIN archive[18].

[18] GIN: Natural Hazards Portal: https://www.natural-hazards.ch/home/about-us/federal-agencies-with-responsibility-for-natural-hazards.html

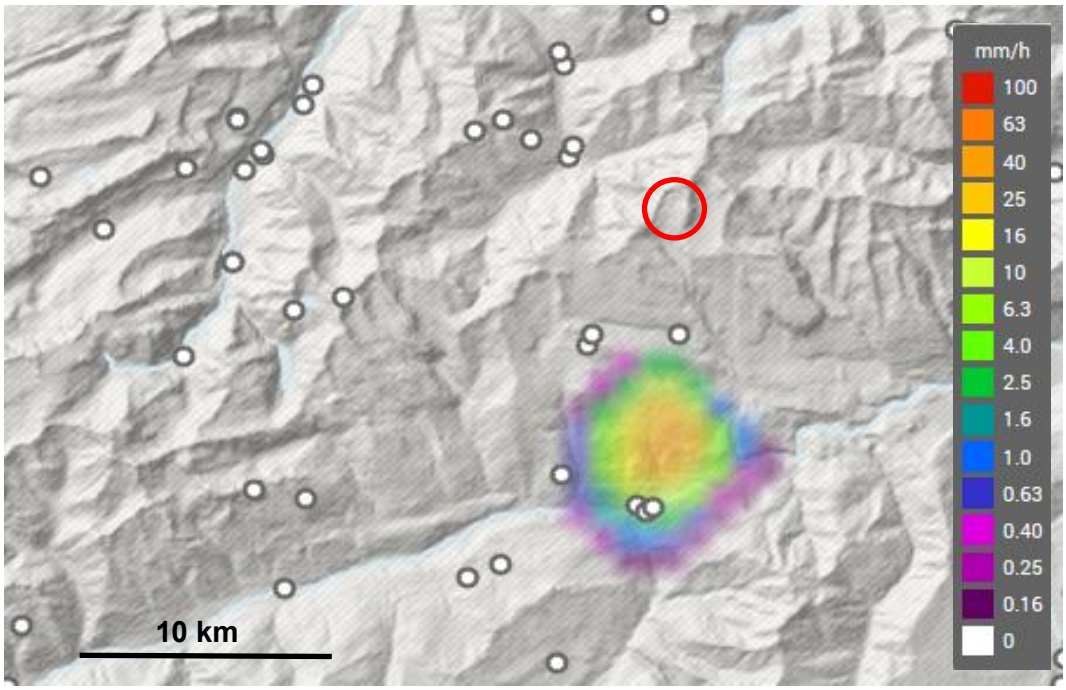

Figure 12: Precipitation radar image at 14:30 LT. The accident happened within the red circle. The small white circles mark the location of surface weather stations. See text below for more information. Source: Federal Office of Meteorology and Climatology, via GIN archive.

Figure 13: The shower at 14:30 near Ilanz as seen by the webcam at Mutta Rodunda[19] (red placemark on the map). The site of the accident is marked by the orange pointer on the image and on the map. The core of the shower (see figure 12) is marked by the blue circle. Source of the map: Federal Office of Topography.

Between 13:50 LT and 15:00 LT, stronger precipitation with up to 25 mm/h was detected near Ilanz, in the vicinity of the later flight. The radar image in figure 12 shows the maximum intensity (orange) during that period at 14:30 LT. This shower is also clearly visible on the webcam between 14:20 LT and 14:40 LT. Figure 13

[19] https://laax.roundshot.com/mutta-rodunda/ (for archive, see calendar icon on the right-hand navigation bar)

shows the shower at the same time that the radar image in figure 12 was generated. This demonstrates the isolated nature of the shower that was generating the prominent radar echo. The visibility outside of the shower remained excellent.

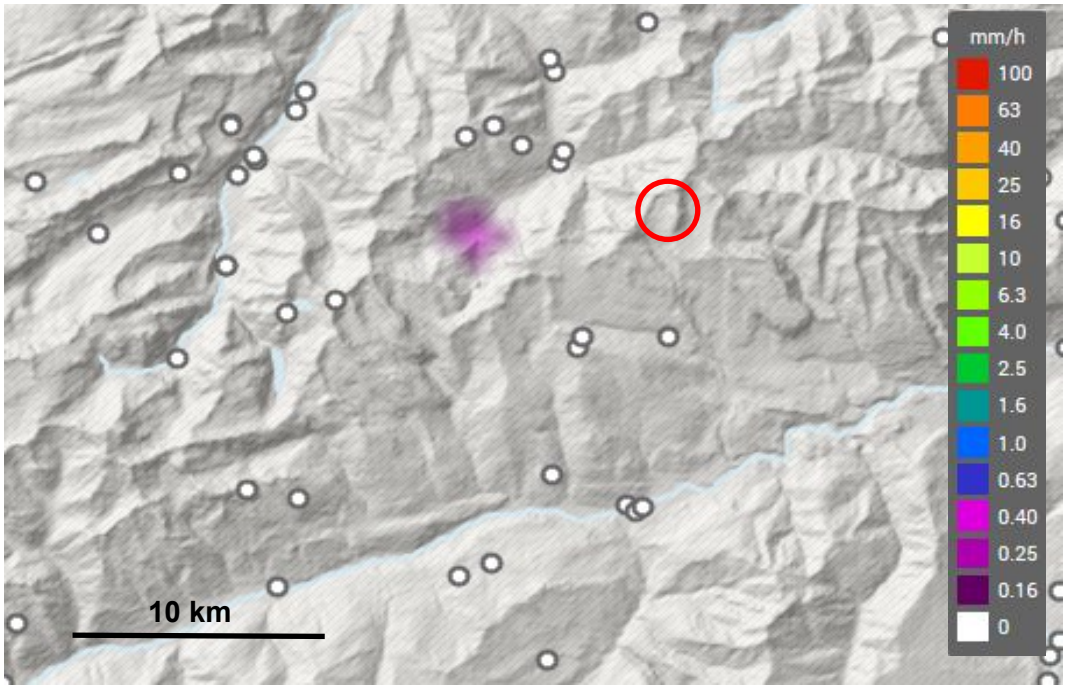

Figure 14: Precipitation radar image at 16:35 LT. The accident happened within the red circle. The small white circles mark the location of surface weather stations. See text below for more information. Source: Federal Office of Meteorology and Climatology, MeteoSwiss, via GIN archive.

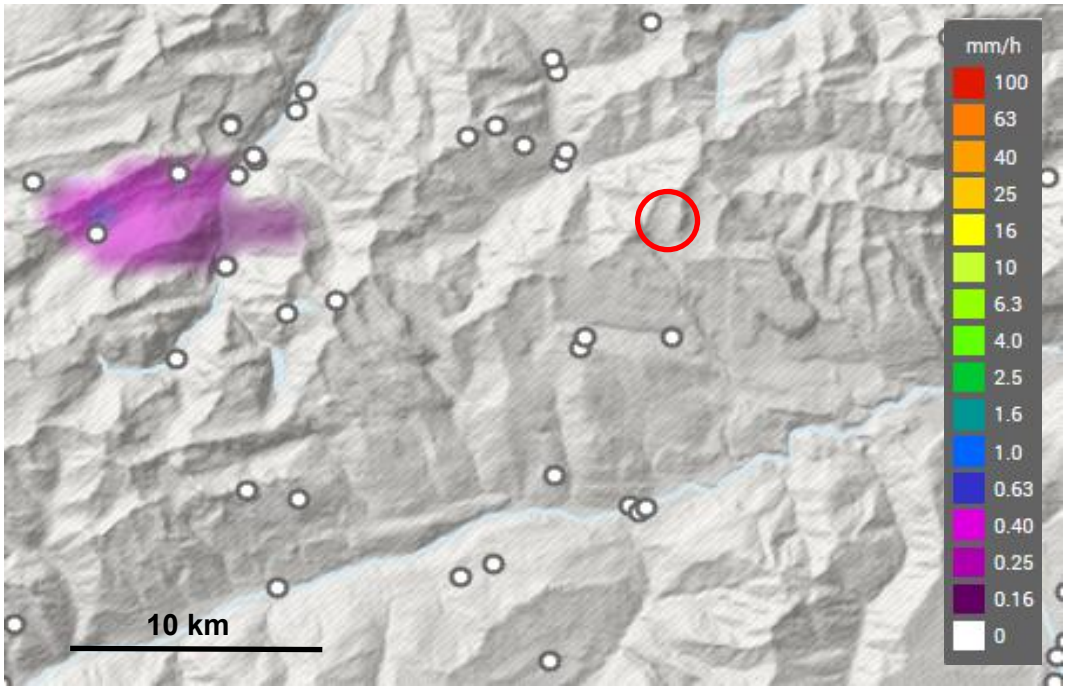

Figure 15: Precipitation radar image at 16:55 LT. The accident happened within the red circle. The small white circles mark the location of surface weather stations. See text below for more information. Source: Federal Office of Meteorology and Climatology, via GIN archive.

Shortly before and at the time of the accident, two weak showers of rain were detected 7 km west, and 15 to 20 km west of the Segnes pass (figures 14 and 15). Both showers were not visible by the webcam because they were behind the crest. However, only TCUs but no CBs are visible above.

A1.7.11 Weather charts, weather stations and balloon soundings

The three types of meteorological information mentioned in this title are essential for analysing a weather situation and creating a forecast. The information from different scales and types of instruments (e.g. according to sections A1.7.9 and A1.7.10) are integrated to form a synoptic view when the national and international weather services are feeding their models with this data (see section A1.7.12).

A1.7.11.1 Weather charts

The general weather situation as it was summarised in section A1.7.1 is characterised by the two charts in figure 16.

The upper air chart for 500 hPa (lower chart in figure 16) shows the centre of a high-pressure system west of Portugal (Azores anticyclone), which extends over Central and Eastern Europe. This pressure field generated northerly winds at about 5,880 m AMSL above the Alps.

The surface chart shows a flat pressure distribution over Central Europe, i.e. the pressure gradients and hence the winds on this scale are weak. However, on a smaller scale, not resolved by this type of chart, regional pressure differences define the wind field at lower altitudes (see section A1.7.13).

A large collection of other charts and numerical products on different scales was also inspected. However, for this general characterisation of the large-scale weather, these two charts are sufficient. More detailed analyses on the regional scale within the Alps are discussed in sections A1.7.12 and A1.7.13.

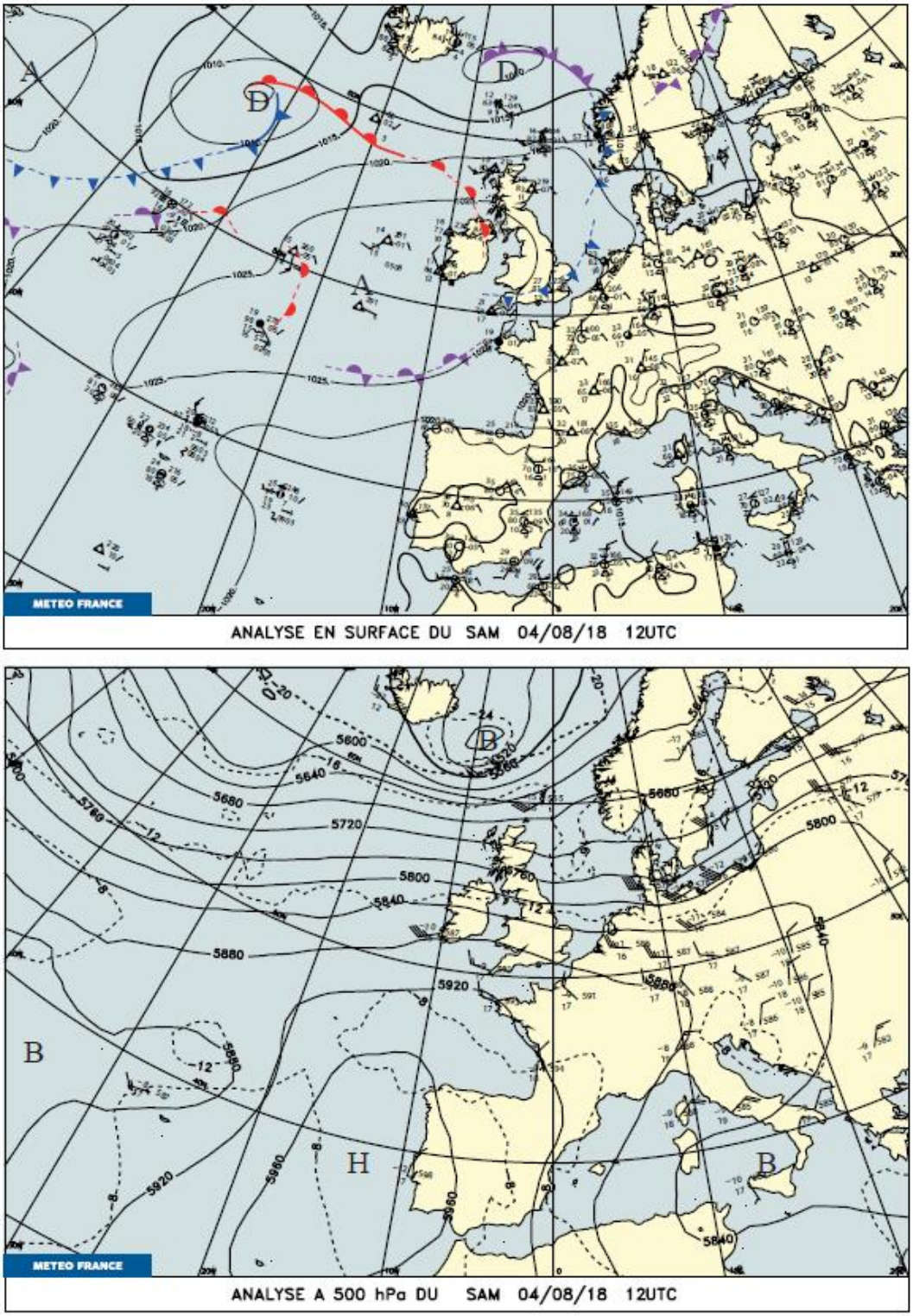

Figure 16: The European surface weather chart (top) and the upper air chart for 500 hPa (bottom). Source: Météo-France.

A1.7.11.2 Weather stations

MeteoSwiss operates a dense network of about 160 automatic surface weather stations. These are documented on its homepage[20]. Most readings are archived in

[20] https://www.meteoswiss.admin.ch/home/measurement-and-forecasting-systems/land-based-stations/automatisches-messnetz.html

intervals of ten minutes. One of the mountaintop stations is Crap Masegn, about 7 km south-west of the accident's site. The recorded measurements from this station were used for this investigation.

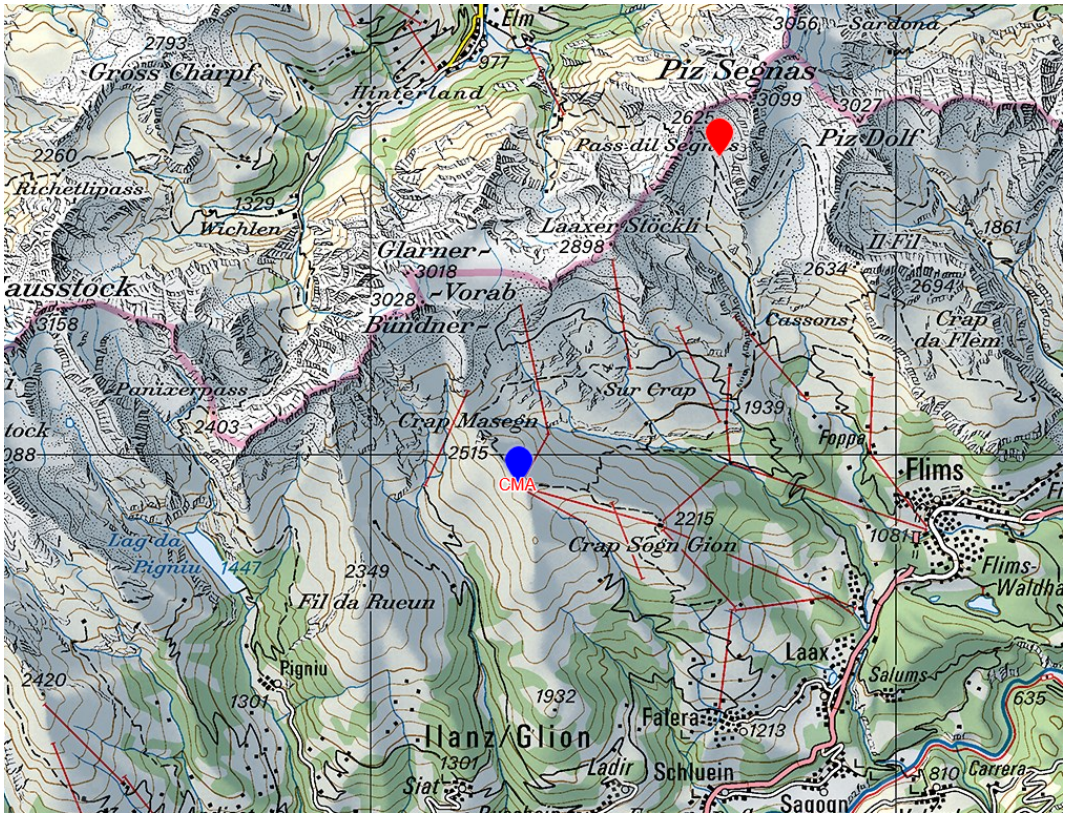

Figure 17: Position of the automatic weather station at Crap Masegn[21] (blue placemark) about 7 km south-west of the accident's site (red placemark), which are on a similar elevation of 2,480 m AMSL. Source of the map: Federal Office of Topography.

The measured values from this station were used in the summary of section A1.7.2. The exposure of Crap Masegn at the southern slope of the northern ridge of the Rhine Valley is comparable to the region south of Piz Segnas.

Table 1 lists the measurements of the wind and other parameters during the afternoon between 14:00 LT and 18:00 LT. This shows the evolution of the wind before the accident happened. The average wind speed from the northern sector (356° to 19°) decreased first from 10.5 m/s down to 5.1 m/s (i.e. from about 20 kt to 10 kt), before increasing again. Gusts with durations of one or three seconds reached about 25 kt within the two 10-minute intervals around the time of the accident (see the graphical display in figure 32).

[21] https://www.meteoswiss.admin.ch/home/measurement-values.html?param=messwerte-lufttemperatur-10min&station=CMA

	wind											
time	veloc.	direct.	gusts 3s	gusts 1s	temp	dew point	QFE	QNH	sun	globrad.	flash n	flash d
h LT	m/s	degree	m/s	m/s	°C	°C	hPa	hPa	%	W/m2	number	number
14:00	10.5	16	12.7	13.0	14.2	7.1	762.5	1031.1	100	1046	0	0
14:10	9.1	12	12.0	13.8	14.2	7.2	762.5	1031.1	100	1010	0	0
14:20	8.9	13	11.1	11.4	14.4	7.5	762.5	1031.1	100	979	0	0
14:30	9.5	18	12.1	13.0	14.5	7.4	762.5	1031.1	100	957	0	0
14:40	8.0	17	10.5	11.2	14.6	7.6	762.6	1031.2	100	941	0	0
14:50	6.3	19	10.2	11.4	14.6	6.8	762.7	1031.3	100	928	0	0
15:00	5.4	6	8.9	9.6	15.1	6.8	762.7	1031.3	100	912	0	0
15:10	7.1	19	10.9	12.9	14.7	7.5	762.6	1031.2	100	892	0	0
15:20	6.5	19	10.6	11.5	14.5	7.2	762.6	1031.2	100	867	0	0
15:30	6.0	12	9.1	9.5	14.7	6.9	762.6	1031.2	100	842	0	0
15:40	5.5	356	10.0	10.7	15.0	7.3	762.5	1031.1	100	835	0	0
15:50	5.1	17	8.7	9.5	14.9	6.8	762.5	1031.1	100	819	0	0
16:00	6.3	11	11.0	11.5	15.0	7.0	762.4	1030.9	100	805	0	0
16:10	7.7	13	10.5	12.2	15.2	6.8	762.3	1030.8	100	790	0	0
16:20	7.8	4	10.7	11.1	15.1	7.1	762.3	1030.8	100	767	0	0
16:30	6.0	6	10.7	11.6	15.0	6.0	762.4	1030.9	100	741	0	0
16:40	7.6	2	12.9	13.3	14.9	6.5	762.4	1030.9	100	713	0	0
16:50	8.2	9	13.0	13.4	14.9	6.7	762.3	1030.8	100	686	0	0
17:00	6.6	6	12.4	12.9	14.8	6.4	762.4	1030.9	100	654	0	0
17:10	7.0	6	12.2	13.4	15.0	6.1	762.4	1030.9	100	627	0	0
17:20	8.1	358	11.8	12.2	15.0	6.8	762.2	1030.7	100	607	0	0
17:30	7.5	4	12.7	13.5	14.9	6.7	762.2	1030.7	100	581	0	0
17:40	8.5	7	11.6	12.4	14.8	6.9	762.1	1030.5	100	521	0	0
17:50	6.5	3	10.8	11.6	14.6	7.6	762.2	1030.7	100	516	0	0
18:00	8.9	19	12.9	13.8	14.7	8.0	762.1	1030.5	100	440	0	0

Table 1: Selected parameters measured in 10-minute intervals between 14:00 and 18:00 LT at the Crap Masegn station. The temperature, dew point and pressure readings QFE[22] and QNH[23] are at the times listed in the first column. All the other parameters are averaged or summed up within the intervals before the given times. The two types of gusts (for 3 or 1 seconds) characterise the maximum wind speed persisting for 3 or 1 seconds, respectively. The intervals around the time of the accident are marked blue. More explanations about the parameters and a discussion can be found in the text below.

The temperature readings show the warm summer conditions at this altitude (16 °C higher than ISA), which is also reflected in the QNH for this reference altitude (see sections A1.7.2 and A1.7.13.2). This high QNH should not be confused with the QNH of the airfields at much lower reference altitudes. The dew point was well below the temperature, i.e. the air was relatively dry. Air pockets rising from this station would condensate at an altitude of about 3,500 m AMSL (cumulus cloud base). However, lower clouds in this region are possible because, in most cases, the cloud base is defined by the temperature and dew point lower in the valley. Based on other information (see section A1.7.12), the cloud base in the region was between 2,800 and 3,400 m AMSL.

100 % 'sun' (sunshine duration for the interval) indicates that no compact clouds south of the station were blocking the direct sunshine. The intensity of the sunshine, including the scattered radiation on a horizontal surface (the global radiation in column 'globrad.') decreases with the descending sun.

Finally, no flashes of lightning were detected near the station ('flash n' < 3 km away from the station) or more distant ('flash d' between 3 and 30 km). Precipitation is not measured at this exposed mountain station (see section A1.7.10 instead).

The relevance of these wind measurements at Crap Masegn for the wind south of the Segnes pass is discussed in section A1.7.14.3.

[22] Pressure measured at the altitude of the barometer (2,482 m AMSL)

[23] Pressure reduced from the altitude of the barometer to sea level by using the ICAO standard atmosphere (ISA)

A1.7.11.3 Balloon soundings

Vertical soundings in the atmosphere using balloons are still the 'backbone' of the global observation system. They are the only tool for establishing the structure of temperature, humidity and wind with the necessary accuracy, precision and vertical resolution worldwide. On the other hand, the horizontal resolution is poor outside of densely populated regions and over the oceans. Furthermore, vertical soundings are only made twice per day in most places (typically at 00:00 and 12:00 UTC[24]). In combination with ground-based measurements (including remote sensing such as radar) plus observations by aircraft[25] and satellites, they provide the basis for weather charts (see section A1.7.11.1) and numerical weather prediction (see section A1.7.12).

The two sounding stations Payerne[26] and Milano are relevant for characterising the atmosphere north and south of the Alps. They are available for the standard times 00:00 and 12:00 UTC (02:00 and 14:00 LT). Considering that the standard times are defined as when the balloons cross the tropopause (i.e. the launches are about one hour earlier), these soundings in figure 18 reflect the state of the lower atmosphere over the Swiss Plateau and the Po Valley for the early afternoon – about three to four hours before the accident. This does not impact the assessment of the thermal stability of the atmosphere, or wind at higher altitudes. However, the regional and local wind at lower altitudes – especially above the complex terrain of the Alps – is affected by short-term changes.

The changes forecast by the numerical weather prediction are expressed in the texts and tables in section A1.7.5.1. The vertical profiles of temperature and humidity are conditionally unstable, which means that the stratification was about neutral below the cumulus cloud base, but unstable as soon as condensation occurred. The consequence of such a stratification is that cumulus clouds – once triggered – will rapidly form into towering cumuli (TCUs) and thunderstorms (CBs) when no other meteorological processes stop them. Such processes exist and are the reason why the development of thunderstorms is different in different regions (see figure 10). On the north side of the Alps, a stable layer around 600 hPa (about 4,500 m AMSL) had to be overpowered.

Figure 18 on the next page: Thermodynamic diagrams show the vertical profiles of temperature, dew point and wind from the Payerne[27] and Milano[28] balloon soundings. The primary vertical coordinate (left-hand axis) is pressure. The altitudes indicated on the right-hand scale in km and 1,000 ft are calculated based on the present state of the atmosphere, i.e. they express true altitudes (not flight levels, FL). The isothermal lines on this skew-T-log-p-diagram (scale on the x-axis) are inclined, parallel to the red 0° isothermals. On both sides of the Alps – and most likely over the Alps as well – the stratification was conditionally unstable (see text). The wind in the north below 3,200 m AMSL was 10 to 15 kt from north-east, turning to north-west and west above. Over Milano, wind speeds of 10 to 15 kt were only observed above about 3,500 m AMSL.

[24] Daily display of worldwide balloon soundings: https://www.ecmwf.int/en/forecasts/charts/monitoring/dcover?facets=undefined&time=2018080412,0,2018080412&obs=Temp&Flag=all

[25] https://www.ecmwf.int/en/forecasts/charts/monitoring/dcover?facets=undefined&time=2018080412,0,2018080412&obs=aircraft&Flag=all

[26] https://www.meteoswiss.admin.ch/home/measurement-and-forecasting-systems/atmosphere/radio-soundings.html

[27] Source: http://weather.uwyo.edu/upperair/bufrraob.shtml, using the software RAOB for a uniform display

[28] Source: http://weather.uwyo.edu/upperair/sounding.html, using the software RAOB for a uniform display

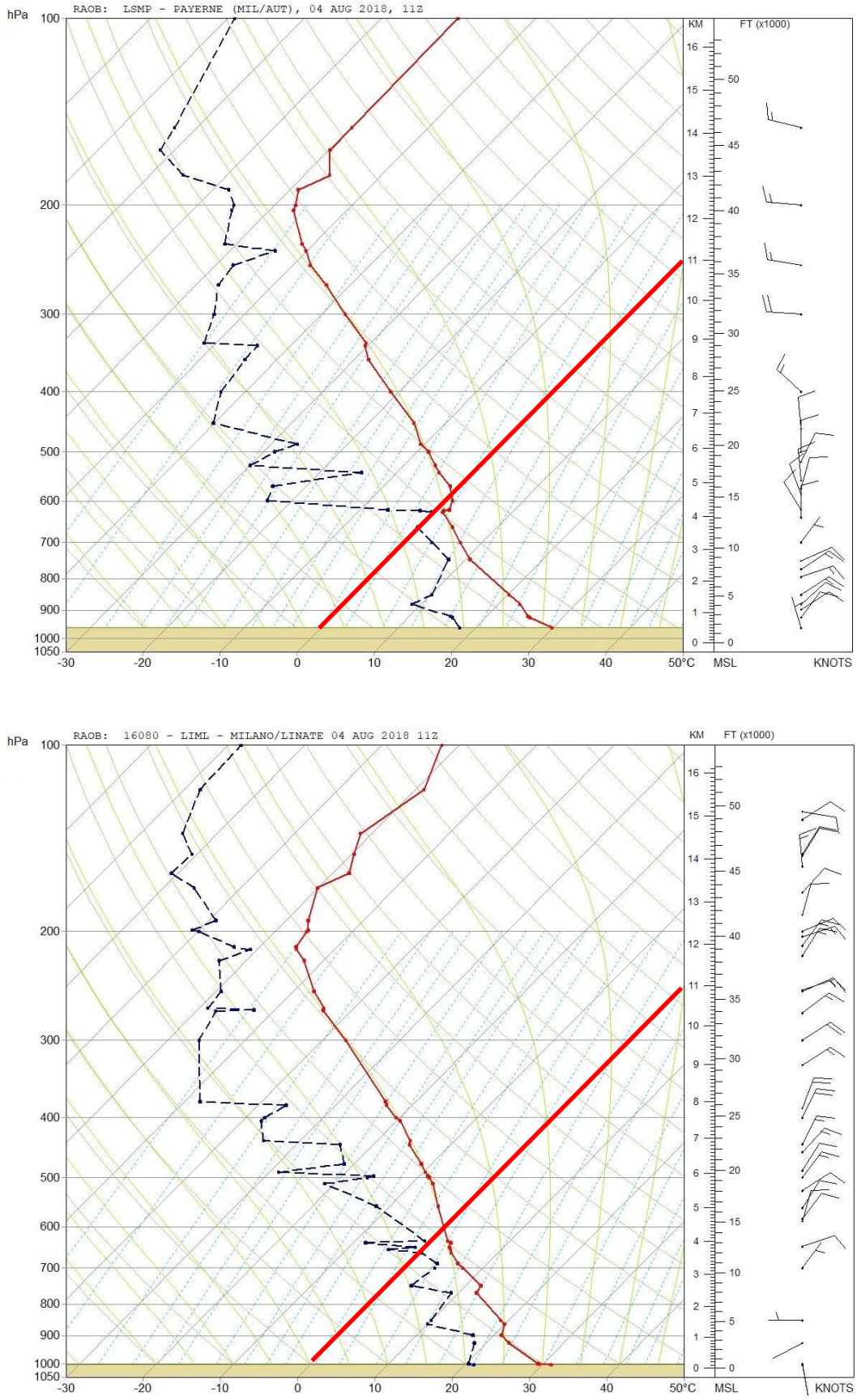

Figure 18: The caption is on the previous page.

A1.7.12 COSMO analyses

Weather stations, balloon soundings and ground-based measurements (see section A1.7.11), plus all the other measurements such as radar and satellite observations, can only characterise the atmospheric conditions over a limited area. They need to be integrated in a suitable way to establish a complete picture of the actual state of the atmosphere. Such a sophisticated integration is called assimilation. This is a crucial step before running a model for numerical weather prediction. The product of the assimilation is a three-dimensional analysis of the present state of the atmosphere. This is much more than a mathematical interpolation of different measurements. Such an analysis creates three-dimensional fields of temperature, humidity, pressure and wind that are physically consistent. They reflect the best estimate for the state of the atmosphere at the time of the observations. These fields are more reliable than forecasts. More information on numerical weather prediction and the COSMO-1 model of MeteoSwiss[29] is available on the websites of the specific weather services.

The hourly analysis from COSMO-1 was used to assess wind and other parameters of the flights of HB-HOT and other aircraft mentioned in the main report on the day of the accident, and the day before. These virtual flights through the gridded data[30] were also used to derive true altitudes from the transponder altitudes (see annex A1.19). In addition, charts for certain altitude or vertical profiles were extracted from the grid. Figure 19 shows the horizontal and vertical wind components at the altitude where HB-HOT entered the side valley south-west of Piz Segnas.

Even when this model analysis is a qualified approximation of the three-dimensional wind field at the time of the accident, the following limitations must be considered. Each value represents about one square kilometre during a certain average time, i.e. it cannot show a true value for the specified time. Based on general knowledge plus the measurements in 2019 (see section A1.7.14) and the fine-mesh model in section A1.7.15, wind speeds in the lowest layers vary typically ± 50% around their average values. This means that a given average wind speed of 10 m/s (about 20 kt) can include everything between 5 and 15 m/s (10 to 30 kt) for a specific moment. This is especially true for the vertical wind component (colour-coded in figure 19). A value of -2 m/s indicates that when flying through this square kilometre, a downdraught of -2 m/s is likely to be experienced, but the individual up- and downdraughts could vary over a wide range (see section A1.7.14.2, figure 28).

[29] https://www.meteoswiss.admin.ch/home/measurement-and-forecasting-systems/warning-and-forecasting-systems/cosmo-forecasting-system.html

[30] Numerical weather prediction models run on three-dimensional grids of different resolution. The horizontal grid spacing in COSMO-1 is about 1 km. The vertical coordinates are terrain-following, i.e. the lowest grid layer is about 10 m above the smoothed surface, with increasing distance between the layers above.

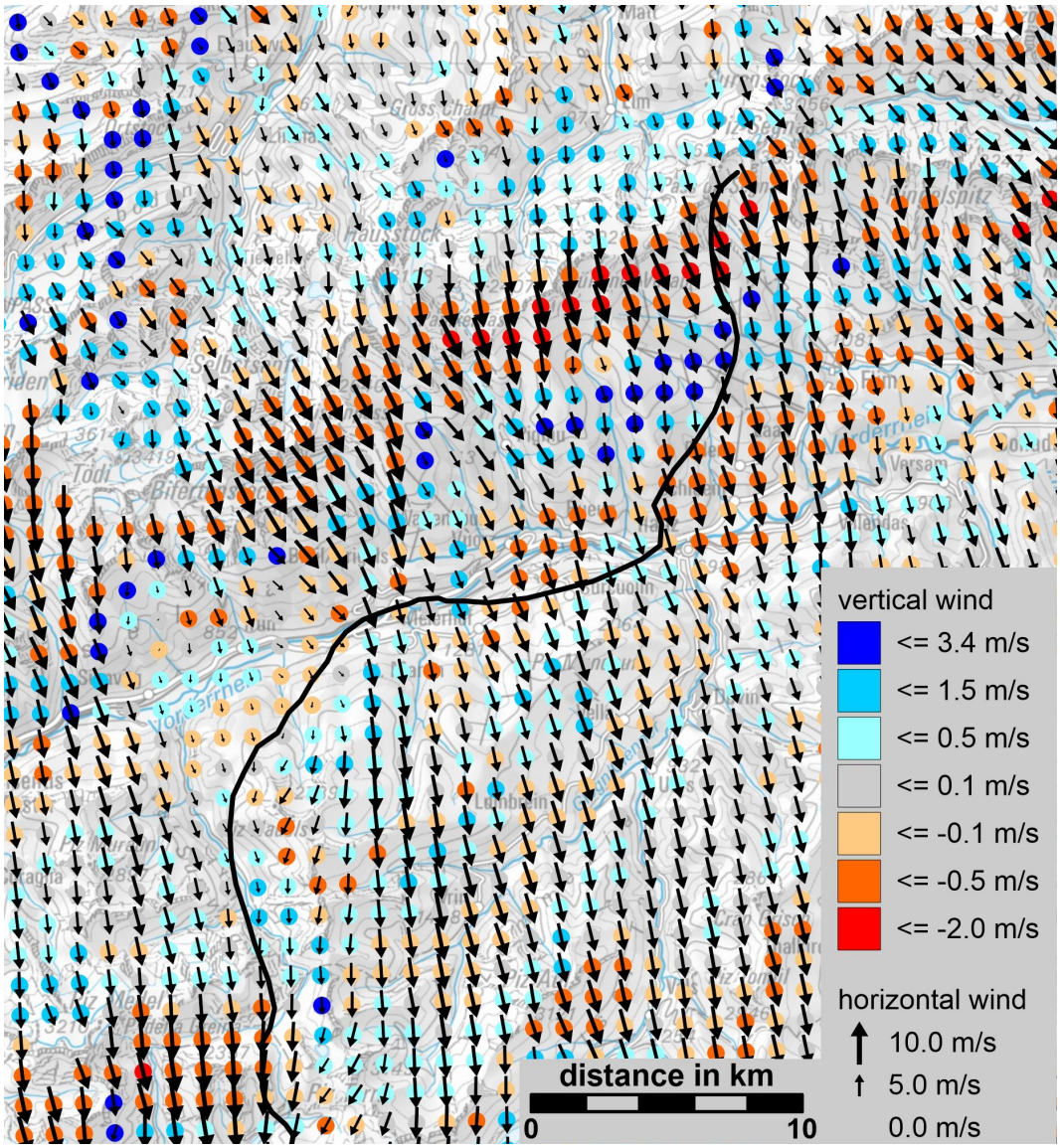

Figure 19: Three-dimensional wind around 17:00 LT at 2,800 m AMSL as interpolated from the terrain-following grid of the COSMO-1 analysis. The coloured points denote the average vertical movement of the air (not individual up- or downdraughts), whereas the arrows show the wind speed and direction (the maximum wind speed on this chart is 10.5 m/s or about 20 kt). The reconstructed flight track is drawn as a black line (see the main report for the official track). Source for the gridded COSMO-1 analysis: Federal Office of Meteorology and Climatology, MeteoSwiss; Source for the background map: Federal Office of Topography.

The conclusions from all this information are discussed in section A1.7.16 and in the main report.

A1.7.13 Regional pressure field

This section summarises basic knowledge about regional wind systems, and how they apply to this particular region.

A1.7.13.1 Theory

Any wind is generated by pressure differences along horizontal distances (= pressure gradients). Since wind moves enormous masses of air (one cubic kilometre has a mass of about a million tonnes), these pressure gradients are not acting instantaneously on the flow, but need a certain time until a new equilibrium with

friction and other forces is established. On a scale of 10 to 100 km, this delay is typically up to one hour. Another important process is the coupling of wind between different layers. For example, turbulent friction between layers accelerates the wind at lower layers when the driving pressure gradient is aloft. On the other hand, the layer in contact with the surface is decelerated by the friction with the rough surface and with obstacles. This process is most pronounced during daytime, when rising thermals and sinking air in between (= convection) are responsible for this coupling of the different layers. Even for advanced models like COSMO-1 (see section A1.7.12) or even PALM (see section A1.7.15), it is still a big challenge to simulate these processes in a realistic way. Therefore, a simulated wind field is usually more reliable 50 to 100 m above the surface than below this height.

Pressure gradients can be caused by different processes on a large scale of 100 km and more. They are defining the pressure systems (highs and lows) that are depicted on weather charts. Below this scale, regional pressure gradients are forming due to different heating, e.g. in different valleys in and around the Alps. Also, different cloud covers over neighbouring areas can cause regional pressure gradients. Such small differences on scales below about 100 km are not captured by the weather charts in figure 16. However, such regional pressure gradients are responsible for thermal wind systems, known as valley and mountain wind, or sea breeze.

The biggest valley in Switzerland is the Swiss Plateau north of the Alps. The air above the plateau is heated less during the day than the air within the Alps. The main reason is pure geometry. While over the plateau, the whole volume of air up to a certain altitude must be heated, about half of the volume is replaced by the terrain within the Alps. The same amount of solar radiation per horizontal area has to heat up less air mass, and the surface of the terrain is absorbing less heat than the replaced volume of air would do. This volume-per-area-effect is especially pronounced near the bottom of valleys and decreases with altitude. Sunny slopes are not a reason for the enhanced heating within the Alps because they are balanced with slopes in shadow. However, there are a few other effects like the drier (and usually clearer) atmosphere over the mountains.

The ambient pressure near the surface and at any altitude above is exerted by the weight of the column of air above. When heating a column of air, this does not change its mass and therefore not the pressure below it. However, the following process takes place. Heating a volume of air causes it to expand by about 0.3 % per centigrade (or Kelvin). When the horizontal expansion is restricted (e.g. in valleys), then the expansion will lift the air above this volume. This means that at the altitude above the heated volume, the pressure is rising, causing the air at this elevated altitude to flow in a direction where the heating is less, i.e. out of the Alps towards the plateau. This reduces the mass of air over the heated valley, leading to a fall in pressure. Even when the heated air in the valley can expand horizontally, mass is lost and the pressure falls. The resulting pressure gradient then drives the valley wind – as it is well-known in the Rhine Valley – between Chur and Disentis, or in the Rhone Valley east of Lake Geneva. These pressure gradients between different Alpine valleys and the foreland can also generate wind across passes like the Segnes pass when the pressure gradients extend up to this altitude.

With an understanding of these basic processes, it can be concluded that valley winds are not produced locally via upslope winds on sunny slopes but are the result of inner Alpine pressure gradients on scales of 10 to 100 km. The same pressure gradients are responsible for accelerated wind across certain passes. By the same reasoning, valley winds in a contradictory direction can develop. The Maloja Wind and a similar wind in the Upper Rhone Valley blow from the more elevated part of their valleys towards the lower sections because the region with the most effective

warming (the centre of the heat island, or the heat low) is situated in the opposite direction than would ordinarily be expected.

These mechanisms are not just restricted to hot summer days but can also cause regional flows in all seasons. However, only when the different warming reaches higher altitudes, are passes affected. Therefore, hot summer days are more prone to accelerated winds across passes and crests than in wintertime with shallow valley winds.

A1.7.13.2 Applying the theory to the Segnes pass

The dense network of meteorological stations in the Swiss Alps allows observation of the diurnal pressure gradients across valleys. Since vertical pressure differences are more pronounced than horizontal ones (typically 1 hPa across 10 m vertical versus 10 to 100 km horizontal), it is not possible to directly compare station readings. For surface weather charts, the pressure readings are reduced to sea level. However, this method is not suitable for the detection of regional pressure differences, because the errors introduced by the reduction are in the same order of magnitude (one or a few hPa) as the horizontal pressure differences of interest, regardless of whether QFF[31] or QNH[32] is chosen for the reduction.

However, this detour via pressure reduction to sea level is not necessary for comparing pressure readings in a certain range of elevations. In this case, it is much better to reduce these pressures to an average elevation in between the stations, or to the elevation of one of the stations. Even the subtraction of a seasonal average pressure for each station results in more realistic horizontal pressure gradients than when reducing to sea level. This recommendation is revisited in section A1.7.16.3. This introduction should allow an understanding of the following discussion.

With this knowledge, suitable weather stations were selected in order to quantify diurnal pressure differences between the Glaronese valleys in the north, and the Rhine Valley south of the Segnes pass. This was not only done for the day of the accident, but for comparable days in August 2018, and in the summer of 2019. ‘Comparable’ does not necessarily mean as hot as between 2 and 5 August 2018, but sunny summer days.

[31] QFF: Pressure reduced to sea level using the local temperature

[32] QNH: Pressure reduced to sea level using ISA, the ICAO Standard Atmosphere (see glossary as well)

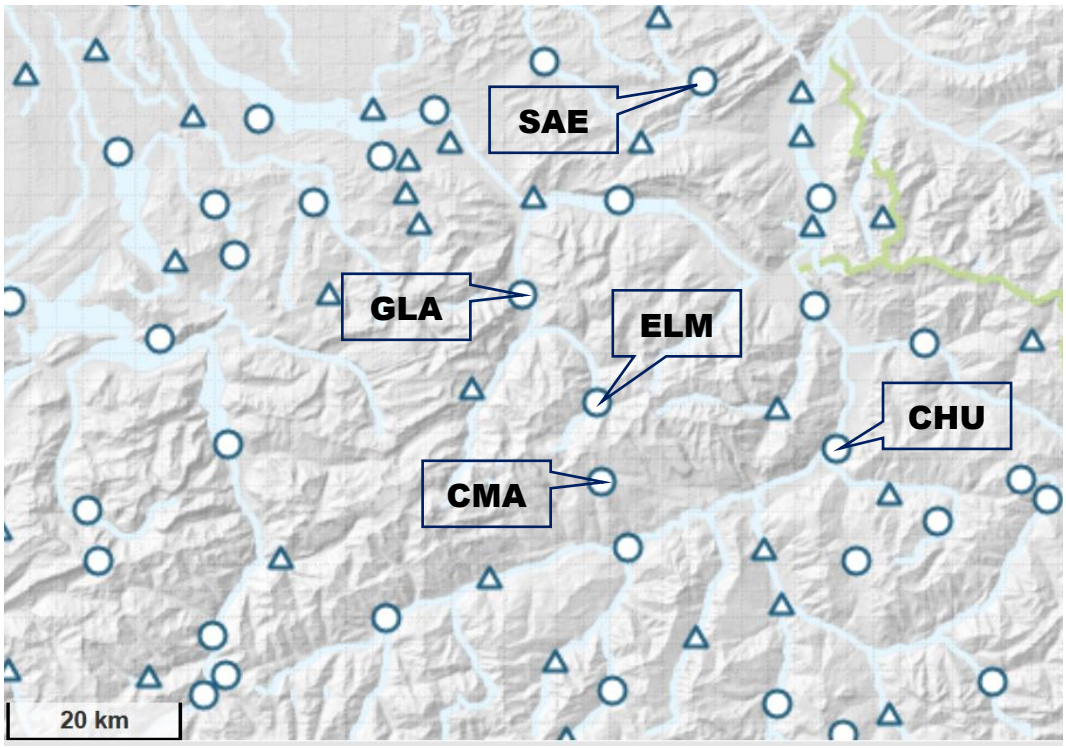

Figure 20: The surface weather stations used in this study – the mountain stations SAE (Säntis) and Crap Masegn (CMA), and the stations on valley floors Glarus (GLA), Elm (ELM) and Chur (CHU). Source and more information about the network of automatic surface weather stations: MeteoSwiss[33].

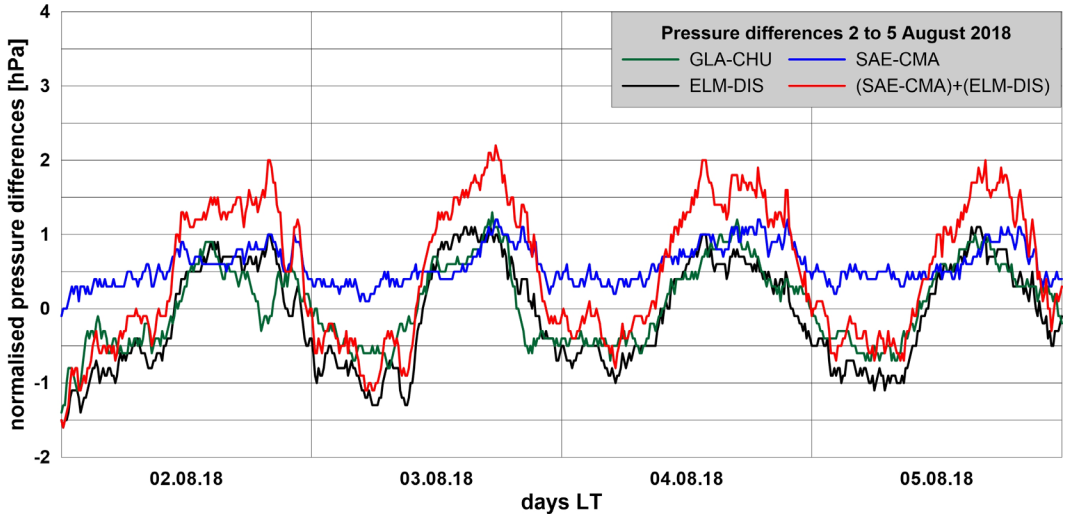

Figure 21: Diurnal pressure differences between selected stations in valleys and on mountains during four days around the day of the accident. See the map in figure 20 for the locations of the stations. Positive values show higher pressure in the north, i.e. from the Swiss Plateau towards the Alps. The pressure at Säntis (SAE) was reduced to the elevation of Crap Masegn (CMA); those at Elm (ELM), Glarus (GLA) and Chur (CHU) to the elevation of Disentis (DIS). The pressure difference SAE-CMA shows pressure differences at the altitude of higher mountains, where ELM-DIS and GLA-CHU show pressure differences between valley floors. The red curve shows the sum of the pressure differences at altitude and the ones between Elm and Disentis. For more information, see the text below.

[33] https://www.meteoswiss.admin.ch/home/measurement-and-forecasting-systems/land-based-stations/automatisches-messnetz.html

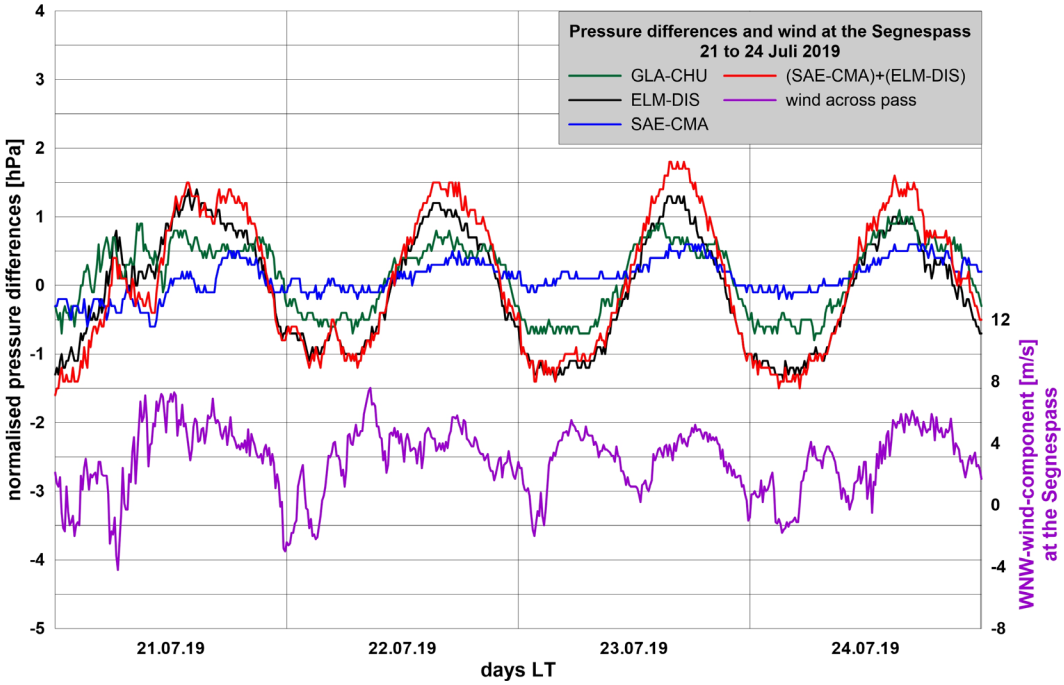

Figure 22: The pressure differences between the same stations as in figure 21, but for four comparable days in July 2019. Since the wind at Segnes pass was measured during that time in 2019, it can be shown in parallel. For more information, see the text below.

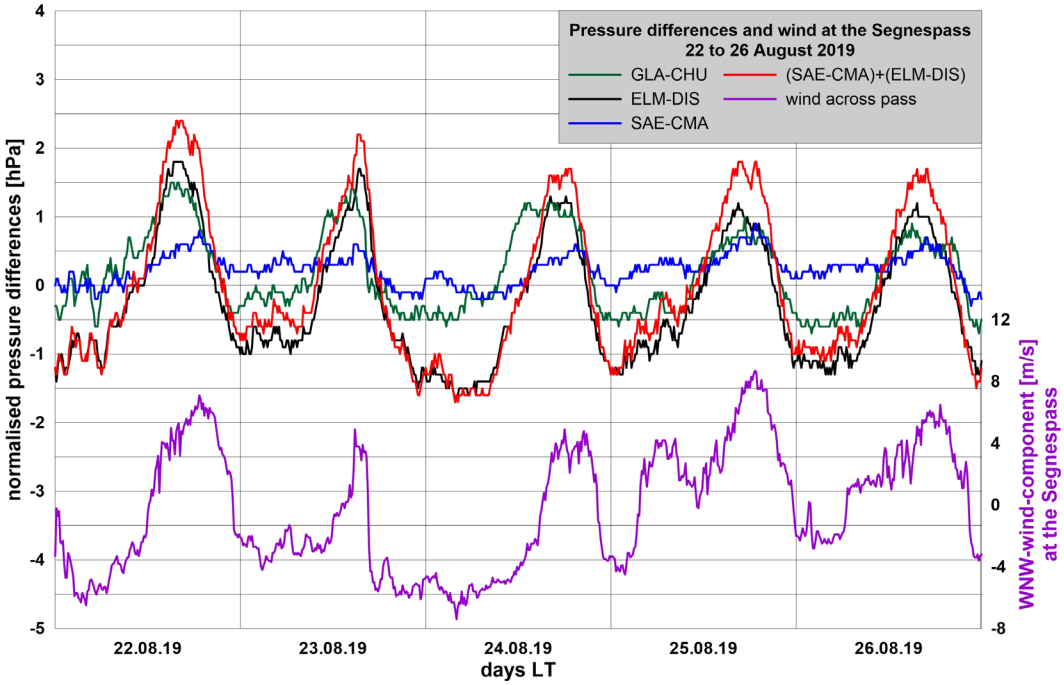

Figure 23: The pressure differences between the same stations as in figure 21, but for five comparable days in August 2019. Since the wind at Segnes pass was measured during that time in 2019, it can be shown in parallel. For more information, see the text below.

The time series in the figures 22 and 23 for nine summer days in 2019 show a similar pattern as during the four days in August 2018. Since the wind across the Segnes pass was measured in 2019 (see section A1.7.14), it can be compared with the diurnal pressure differences.

A typical diurnal pattern can be observed for these days. The pressure differences between Elm in the north and Disentis south of the Segnes pass increase during

the afternoon. The differences are less pronounced at the altitude of the mountain peaks, but still clearly detectable. Additional stations were also inspected, but those selected here seem to be the best choice for documenting the effect of differential heating in neighbouring valleys and aloft. The sum of the pressure difference at lower and higher level is a combined indicator for the enhanced pressure in the north (red curves in figures 21 to 23).

A pressure difference of 1 hPa along less than 50 km (SAE-CMA) is sufficient for the acceleration of the air mass in between, i.e. to generate wind (7 kt after half an hour when calculated without friction). Of course, the even larger pressure differences between valley floors cannot act through the mountains. However, they drive the valley wind systems within the Alps. The comparison of the pressure differences with the wind across the Segnes pass, as measured in 2019 (figures 22 and 23), suggests that the diurnal pressure gradient does indeed drive wind across the Segnes pass as a shortcut.

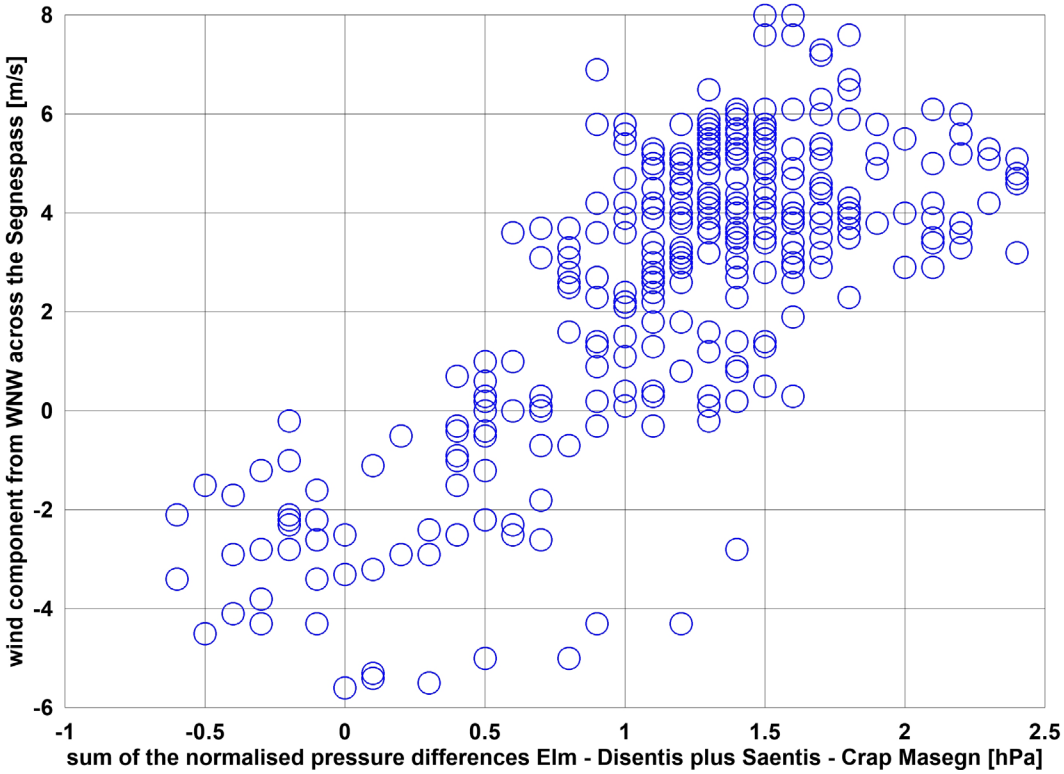

Figure 24: Scatter plot of wind speed across the Segnes pass against the sum of the pressure differences (red curves in figures 22 and 23) between 13:00 and 18:00 LT.

Even when the time series of wind and pressure differences look parallel, and the correlation is visible in figure 24, the relationship is not sharp. It is not possible to forecast an accurate wind speed across the pass based only on this pressure difference. The difference needs to be at least 1.5 hPa to define the direction of the flow. This is due to several reasons: (i) as explained in the theory, the pressure difference is not acting instantaneously; (ii) the wind aloft had different speed and directions during the nine selected days. The wind across the pass is a result of the upper-level wind, and the additional acceleration by the regional pressure gradient. During the sample days in 2019, the wind aloft did not reach the 10 or even 15 kt from the north as it did on 4 August 2018. Nevertheless, this additional contribution by the regional pressure gradient is quite important and robust.

This study shows that during sunny days in the summer of 2019, a north-westerly flow established across the Segnes pass, as a result of the diurnal pressure difference between the Glaronese valleys in the north and the Rhine Valley.

It is obvious that such a flow will be amplified when the synoptic wind from above is blowing from a northerly direction. Cooler air near the surface from the northern slope can additionally accelerate the downwind flow of the pass (see section A1.7.7).

All the processes described and analysed here are included in the numerical weather prediction model COSMO-1 as it was introduced in section A1.7.12. However, the basic theory in section A1.7.13 and the discussion of the measurements presented some additional empirical evidence.

The relevance of the wind and turbulence at the time of the accident is discussed in section A1.7.16.2.

A1.7.14 Meteorological measurements around the Segnes pass

The exact wind conditions along the flight of HB-HOT can neither be reproduced by measurements, nor by models. However, both can define typical patterns of the three-dimensional wind along the final minutes of the flight. Therefore, specific measurements were performed in the summer of 2019 (17 July to 14 September). The aim was to document wind and turbulence near the surface and at the altitude of the flight during conditions that were comparable with the day of the accident.

A1.7.14.1 Wind on the Segnes pass

A typical meteorological station was installed near the Segnes pass Mountain Lodge slightly east of the pass. It measured wind speed, wind direction, temperature and humidity on a six-metre-long pole at 2,650 m AMSL. This location allowed for the documentation of the direction of the flow across the pass, and typical wind speeds, even when such a measurement was influenced by the rocks at this place. The results from these measurements and their correlation with regional pressure gradients are discussed in section A1.7.13.

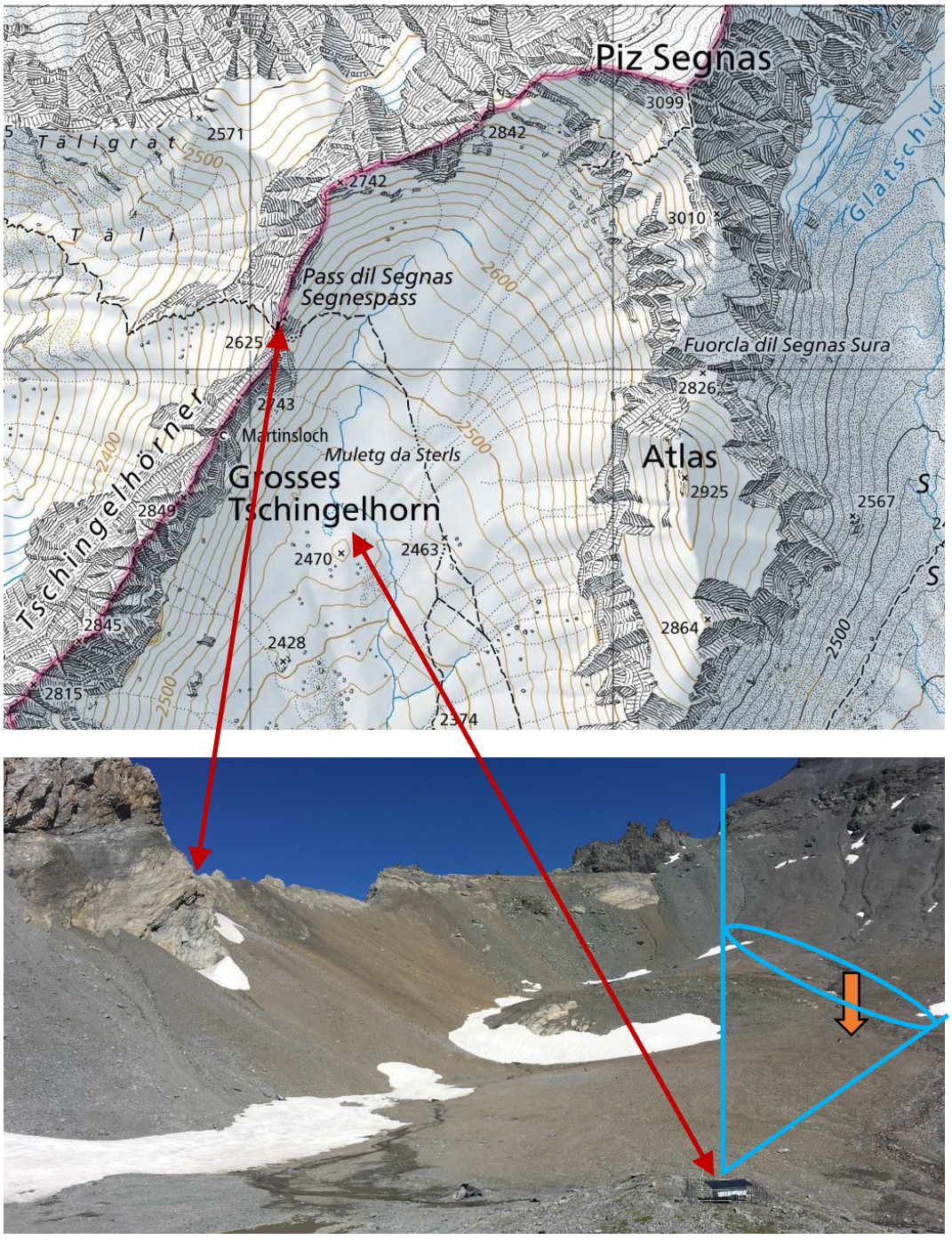

Figure 25: The positions of the meteorological station on the Segnes pass and the wind lidar[34] on a small hill not far from the site of the accident (orange pointer). The light blue lines denote the conical-shaped zone within which the lidar scans the sky up to a height of 200 m (see section A1.7.14.2). Source of the map: Federal Office of Topography.

On the following two pages, the recordings of wind, temperature and humidity are depicted for the seven weeks of the observations.

[34] Lidar: Light detection and ranging

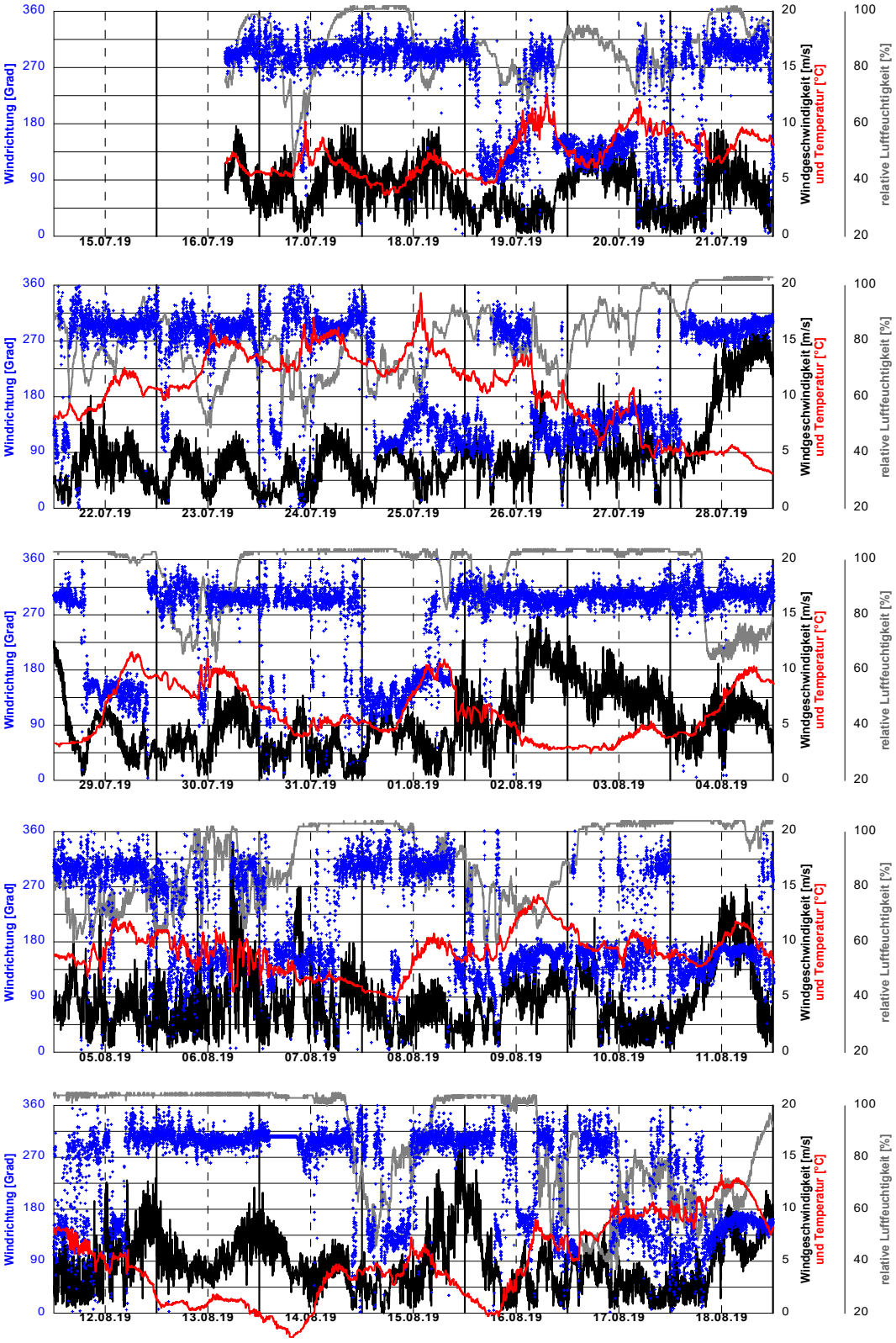

Figure 26: Seven weeks of measurements on the Segnes pass (for weeks 6 and 7, see next page). The vertical dashed lines mark local noon (12:00 LT). The black curves show the wind speed (‘*Windgeschwindigkeit*’, one-minute averages) on the first right-hand scale (10 m/s correspond to about 20 kt). The blue dots indicate the wind direction (‘*Windrichtung*’) on the left-hand scale. The red curve shows the temperature on the same scale as the wind speed. The grey line shows the relative humidity (‘*rlative Luftfeuchtigkeit*’) on the outer right-hand scale. Values around or above 100 % indicate clouds on the pass.

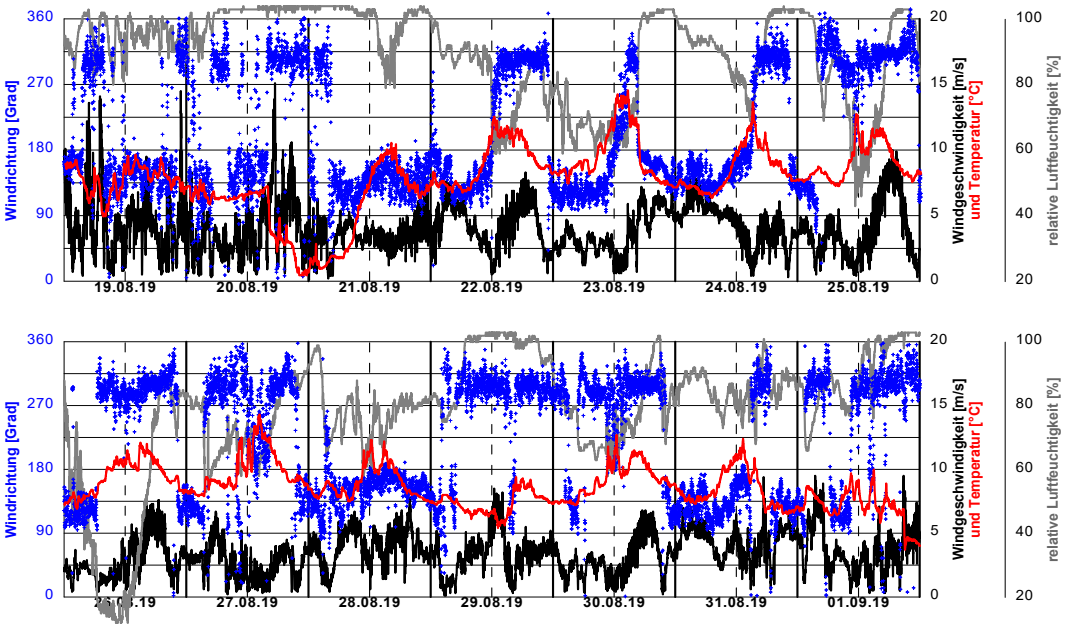

Figure 26, continued: See the caption on the previous page.

This time series shows that the wind across the Segnes pass during the afternoons was regularly blowing from the north-west. The velocities reached 5 to 10 m/s (10 to 20 kt) even close to the surface (6-m pole on a rock).

The summer of 2019 was less dry than the summer of 2018, and a synoptic wind aloft (not displayed here) was missing during the sunny days in this period in 2019. However, 13 days were identified as being comparable with 4 August 2018. The day of 25 August 2019 was ranked as the best, even though there was no stronger northerly wind above.

A1.7.14.2 Wind lidar below the Segnes pass

The measurements on the Segnes pass alone would not be sufficient to assess wind and turbulence along the flight of HB-HOT. However, a wind lidar can fill this gap by measuring the three-dimensional wind at high temporal resolution just below the flight track.

The wind lidar system[35] used here is designed for measuring wind in a relatively small volume above the instrument. It allows the measurement of wind and turbulence with a good spatial and temporal resolution: one wind vector per second at seven different heights, within a range of 10 to 200 m.

The laser scans around the cone outlined in figure 25. While doing this, it measures the radial speed of the air (the speed towards or away from the lidar) in a chosen distance 50 times per second. Despite the high accuracy (<0.2 m/s) of these raw Doppler measurements, the accuracy of the wind vectors calculated within the cone is limited by secondary geometrical and optical effects. Therefore, the lidar was installed in a way that one side of the cone was exactly vertical. This tilted installation and an optimisation of the software allowed for the most reliable measurement of the vertical wind component.

Wind, temperature and pressure close to the surface were measured on a small 2-m pole near the lidar. The time series of wind and temperature are shown in the same manner as the station readings from the Segnes pass.

[35] https://www.zxlidars.com/wind-lidars/zx-300/

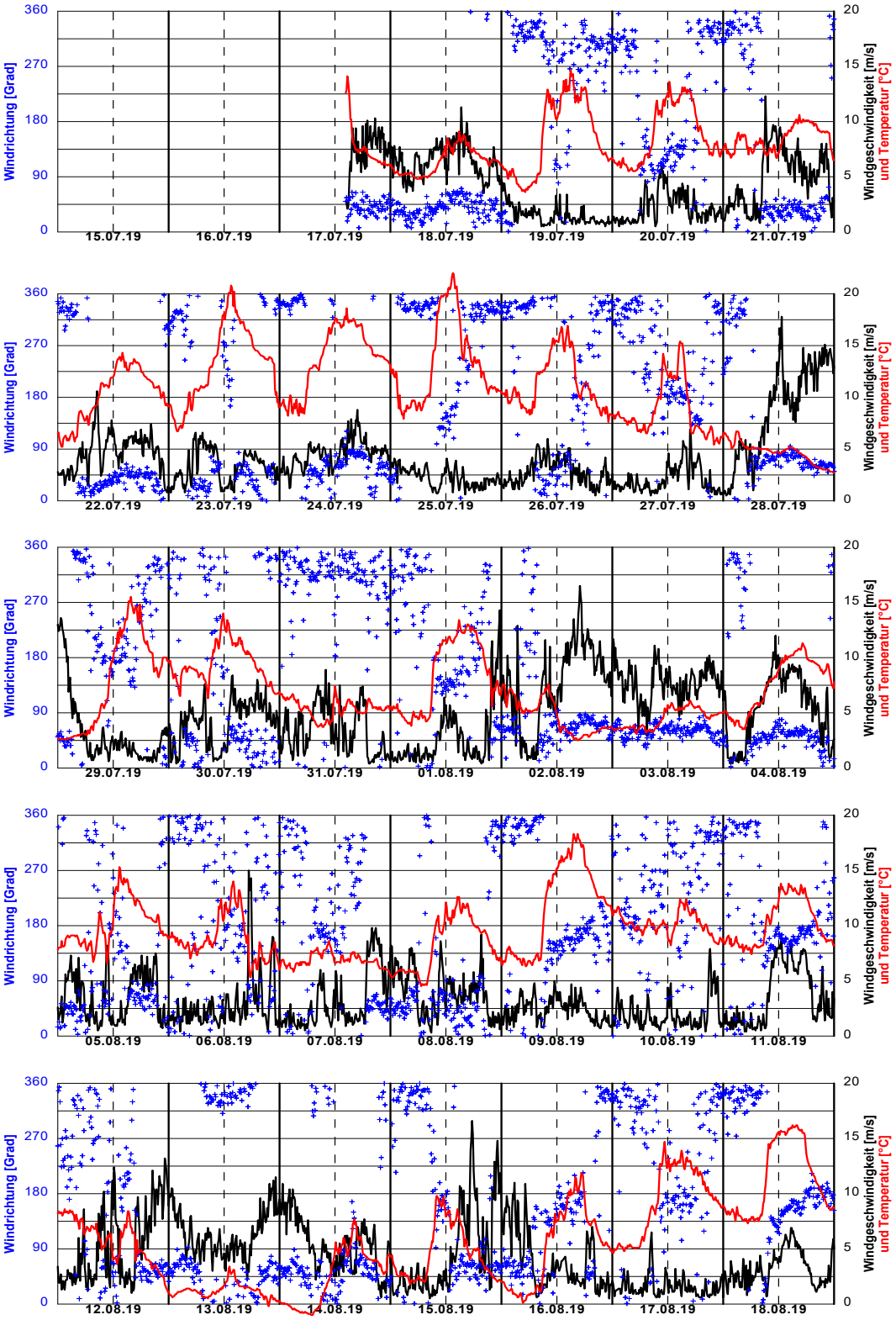

Figure 27: Seven weeks of measurements on the 2-m pole near the lidar (for weeks 6 and 7, see next page). The vertical dashed lines mark local noon (12:00 LT). The black curves show the wind speed ('*Windgeschwindigkeit*', ten-minute averages) on the right-hand scale (10 m/s corresponds to about 20 kt). The blue dots indicate the wind direction ('*Windrichtung*') on the left-hand scale. The red curve shows the temperature on the same scale as the wind speed.

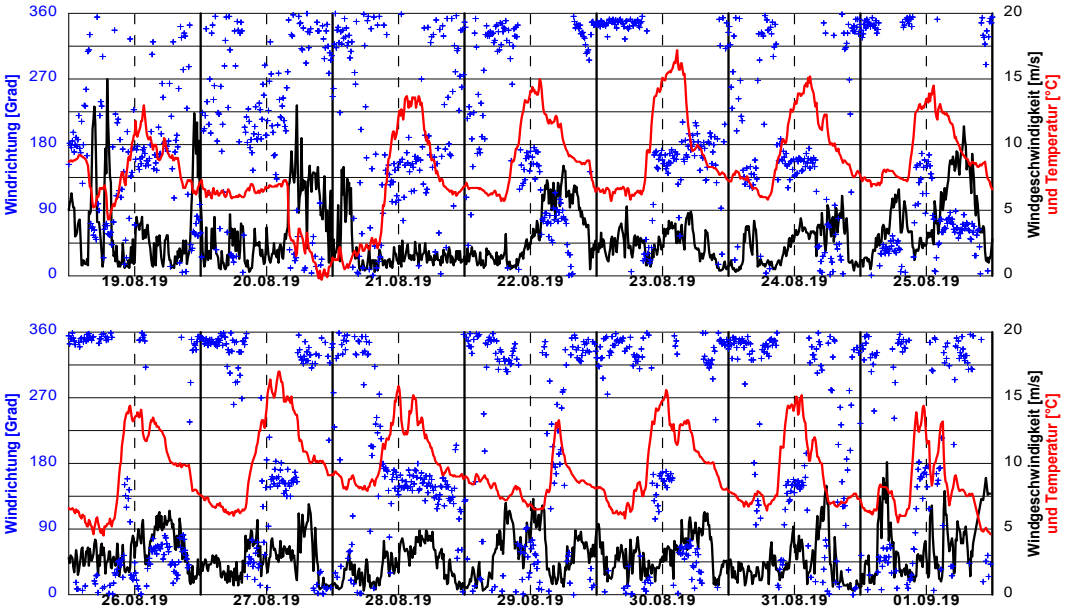

Figure 27, continued: See the caption on the previous page.

These additional measurements close to the surface document the typical occurrence of strong winds from the direction of Piz Segnas during afternoons. During several visits to the lidar station, the significant change between soft upslope winds around noon, and a cooler downslope wind shortly after this phase was also experienced subjectively. These measurements at the southern slope of the pass confirm that 25 August 2019 was the best day for comparison with 4 August 2018.

The lidar also recorded horizontal winds at seven heights within 10 and 200 m. However, due to the above-mentioned secondary effects, these are unreliable in this very heterogeneous flow such as rotors. Therefore, the focus of this study is on the reliable and more relevant vertical wind and turbulence measurements.

Figure 28 shows the time series of the vertical wind for the afternoon of 25 August 2019. The blue curve shows the vertical wind at an altitude of about 2,660 m AMSL, i.e. 50 to 100 m below the flight track of HB-HOT one year previously. Another 12 suitable days were identified for a statistical characterisation of the turbulence in this sector of the valley.

The vertical wind reflects the same diurnal evolution as discussed above for the wind near the surface. Shortly after noon, following a period with some turbulence caused by rising thermals (slope convection with positive vertical gusts between 1 and 3 m/s), stronger negative values were dominant. Based on the station readings from above, this was within the downslope flow from about 60° (see figure 27 for 25 August 2019). Between about 15:00 and 18:00 LT, the vertical wind varied between -6 m/s and +4 m/s.

The mechanisms generating this turbulence (thermals and rotors behind the ridges) during the afternoon suggest that the vertical wind speeds were not very sensitive to altitude, i.e. they would be the same 100 m higher. As such, the measurements taken one year later should not be projected directly to the day of the accident. The measurements describe typical conditions in a statistical way.

The primary question is: how often do such fast changes between downdraughts and updraughts occur within the flow at this location?

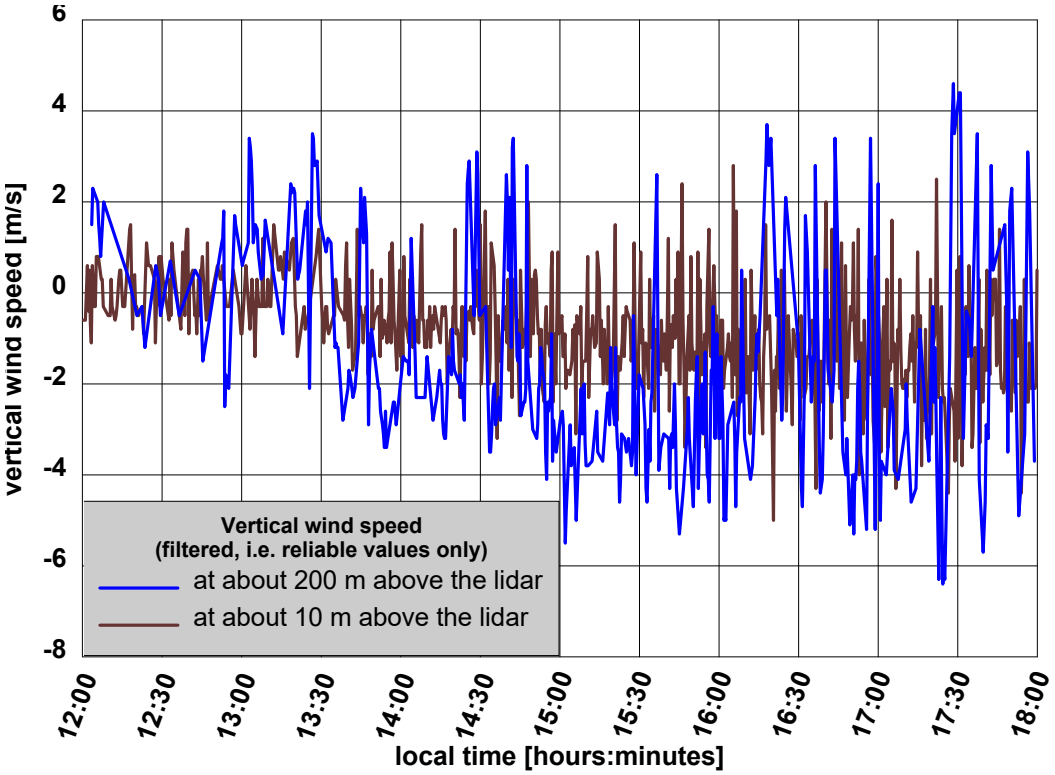

Figure 28: Time series of the vertical wind speeds (positive values are updraughts) at the lowest and highest altitudes measured during the afternoon of 25 August 2019. The 10 and 200 m above the lidar are at about 2,470 and 2,660 m AMSL respectively (8,100 and 8,700 ft AMSL, i.e. about 50 to 100 m below the flight track one year ago). In between these heights, five others were measured and processed. For further information, see the text below.

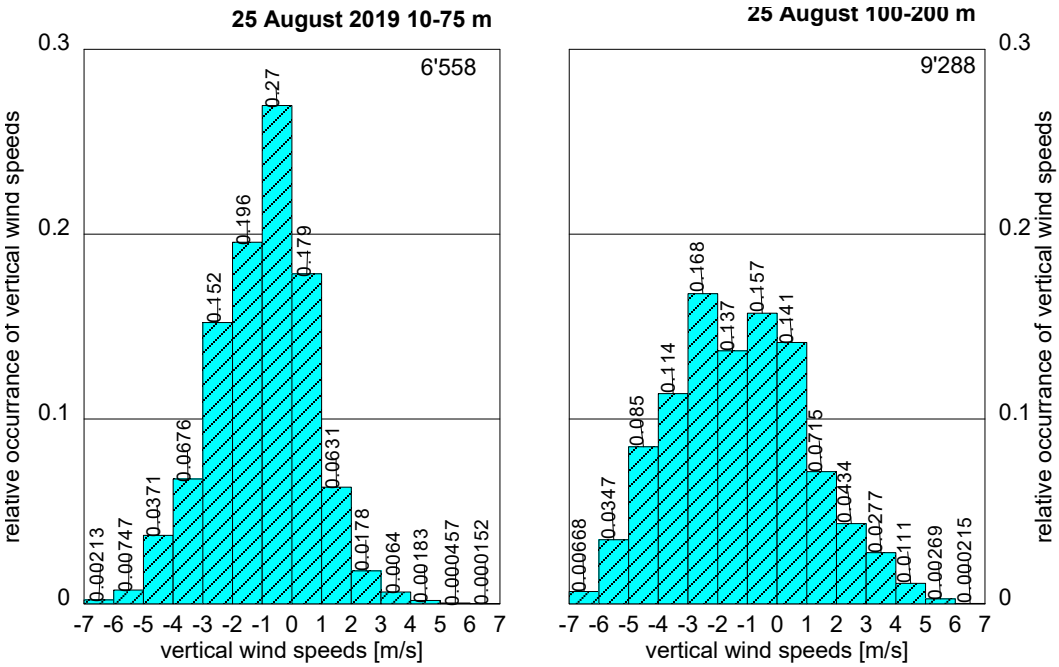

Figure 29: Histograms of the distribution of vertical wind speeds during the afternoon of 25 August 2019 (12:00–18:00 LT) in two height ranges above the lidar: 10 to 75 m (left) and 100 to 200 m (right). The numbers in the top-right corners are the numbers of individual measurements. The vertical axis and the values on top of the bars indicate the relative occurrence, i.e. downdraughts between -2 and -3 m/s dominated with 16.8 % occurrence in the range between 100 and 200 m above the lidar.

Such a statistical evaluation was made with all the 13 days that were selected. An example is presented in figure 29. The bars in the histograms indicate the relative occurrence of the different ranges of up- and downdraughts. At heights below 100 m above the lidar, weak downdraughts dominated with 27 %. Stronger up- and downdraughts exceeding ±3 m/s were encountered more frequently higher up. This is plausible and supports the assumption that these values will not be much different another 50 to 100 m higher up (where HB-HOT flew through a year ago). Even 8.5 % of downdraughts ranging between - 4 and - 5 m/s were detected, and - 5 to - 6 m/s occurred during 3.5 % of the observation time. Updraughts exceeding 3 m/s were found in 3.7 % of the time (sum of all ranges > 3 m/s).

Finally, the question is: how often did fast changes between down- and updraughts occur (because the horizontal shear of the vertical wind speed was a key parameter for the analysis of the accident)? For this purpose, all reliable vertical wind measurements on 25 August 2019 in the higher altitude range were examined. With the assumption that an aircraft flies through this sequence of vertical winds with a true airspeed of 50 m/s, the following probabilities were found for steps of at least 5 m/s (positive or negative) within 3 or 5 seconds, respectively: 1.0 % and 1.8 %. The consequences of these probabilities are discussed in section A1.7.16.2.

A1.7.14.3 Comparison with the operational measurements

As introduced in section A1.7.11.2, the well-exposed meteorological station Crap Masegn 7 km south-west of the accident is considered to be representative for the wind south of the ridge. For the observation period in the summer of 2019, these measurements can be compared with those on the Segnes pass, and at the lidar station below the flight track. An additional measuring station was operated by Flims Electric AG about 4 km south of the accident on an elevation of 2,100 m AMSL, near the Segneshütte mountain restaurant at the southern edge of the Segnas Sut high plateau. Wind and temperature data from this station was available both for 2018 and 2019.

Figure 31 shows the onset of the downslope wind during 4 August 2018, which was stronger than the day before. Ahead of the increasing afternoon winds, periods of weak winds are identifiable, most likely due to initial upslope winds, as discussed in A1.7.14.2. During the afternoons, the downslope winds dominated at this lower station in the same way as higher up in this side valley south of the Segnes pass. During the night before 4 August 2018, a reasonably intensive shower was recorded. The weak shower at 12:50 LT, that is visible on the radar imagery in figure 11, clearly also reached the high plateau, even though the radar echo near Ilanz was smaller. Vice versa, the stronger shower at Ilanz at 14:30 LT (see figures 12 and 13) did not reach the station of Flims Electric. In summary, these precipitation events in the very dry season led to a patchy distribution of soil moisture that enhanced the contrasts in thermal activity and supported the formation of cumuli above the local crests.

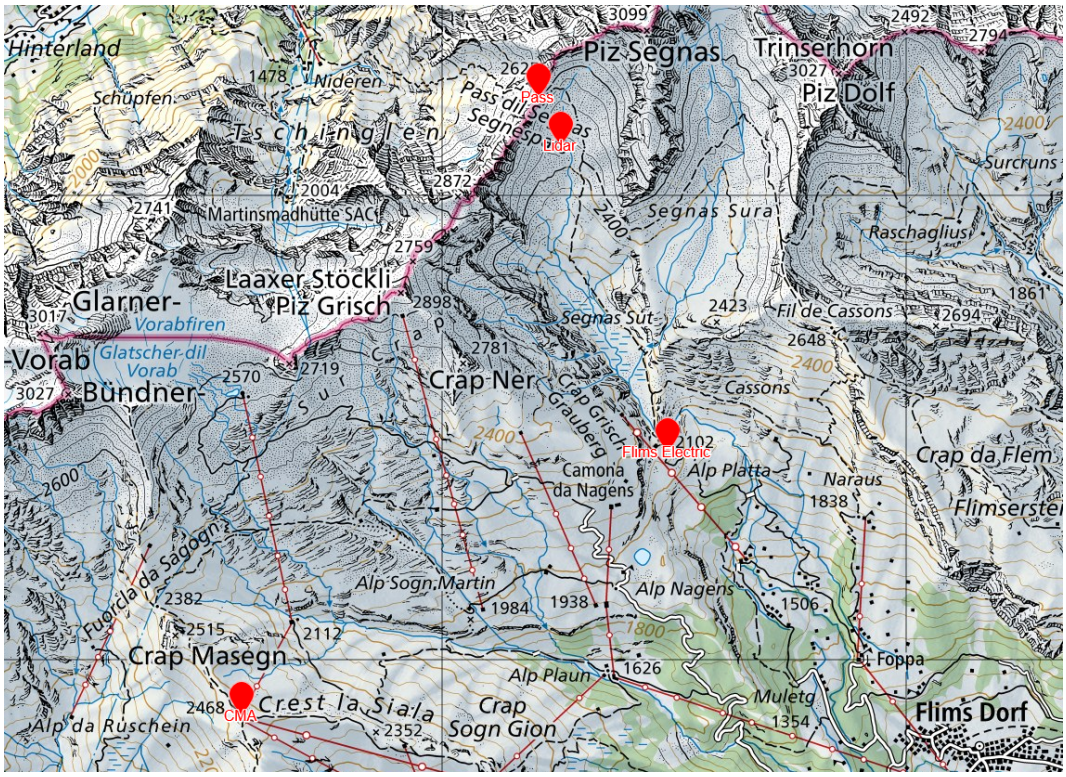

Figure 30: The four meteorological stations discussed in this section. Source of the map: Federal Office of Topography; station CMA see section A1.7.11.2).

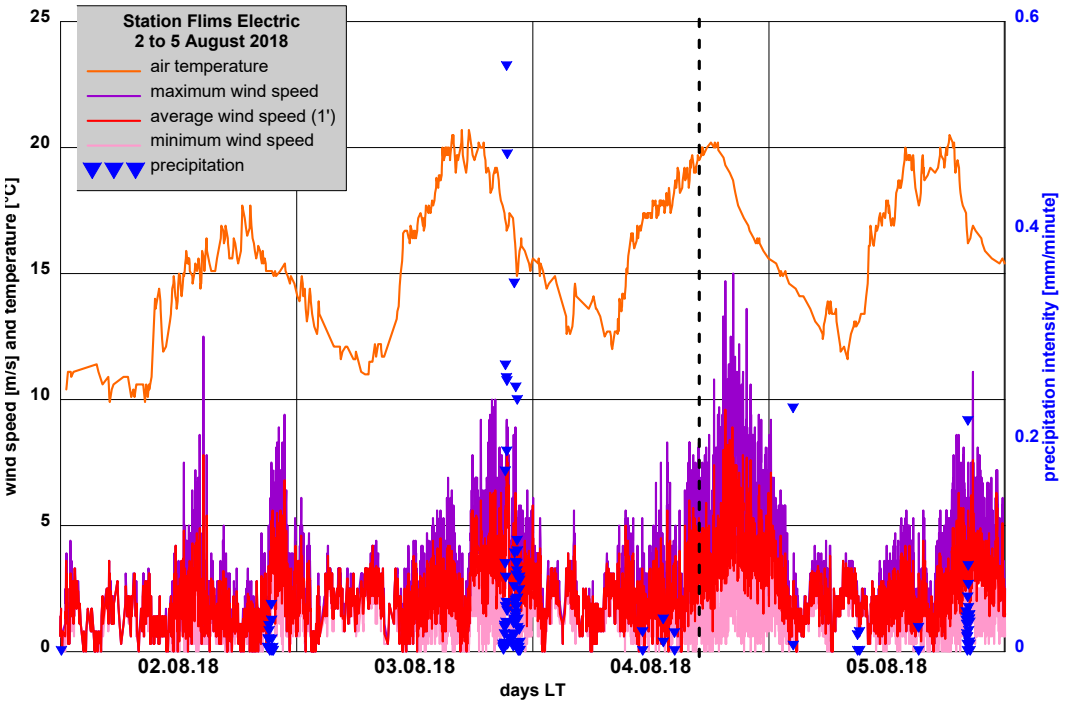

Figure 31: Wind, temperature and precipitation about 4 km south of the accident site at an elevation of 2,100 m AMSL (black dashed line at the time of the accident). The red curve shows the one-minute averages of the wind speed (5 m/s correspond to about 10 kt), whereas pink and purple indicate minima and maxima within the minutes. The wind direction was not recorded but confirmed by the operator to be downslope during the afternoons. The orange curve is for the temperature, and the blue triangles indicate rain according to the right-hand scale (mm/min to be multiplied by 60 for mm/h).

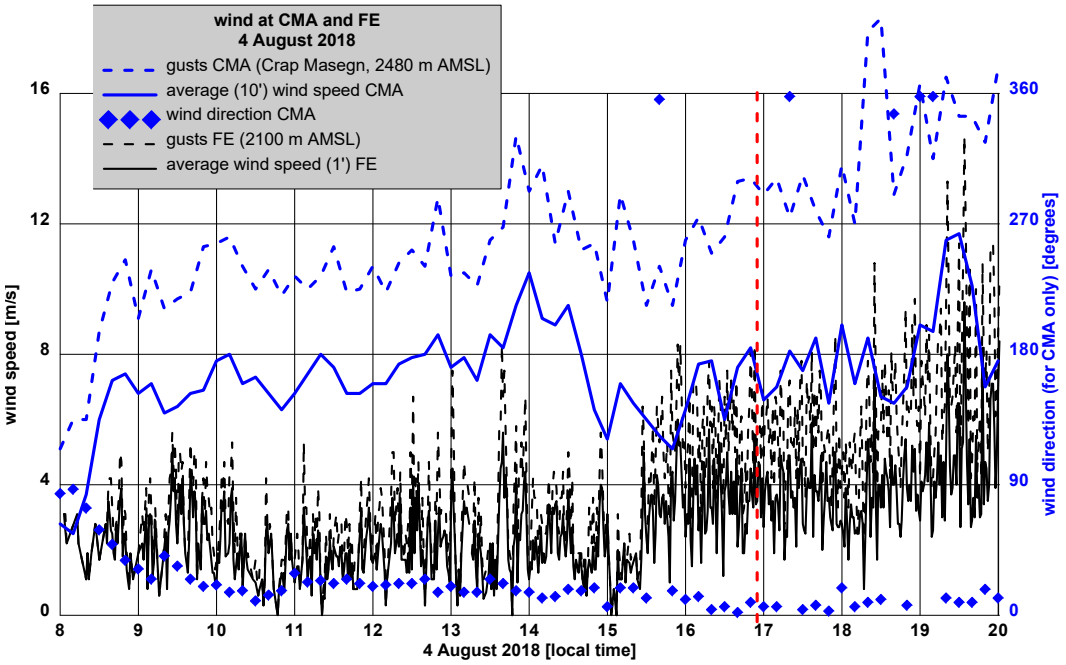

Figure 32: Wind at the two stations Crap Masegn (CMA) and Flims Electric (FE) on the day of the accident. The blue curves and points are for CMA (solid line: 10-minute averages of wind speed; dashed line: 1-second gusts; diamonds: wind direction on the right-hand scale). The one-minute averages and maxima are shown as solid and dashed lines in black. 8 m/s correspond to about 16 kt. Both the average wind speed and the gusts at CMA are about twice as high as at the FE station below the high plateau.

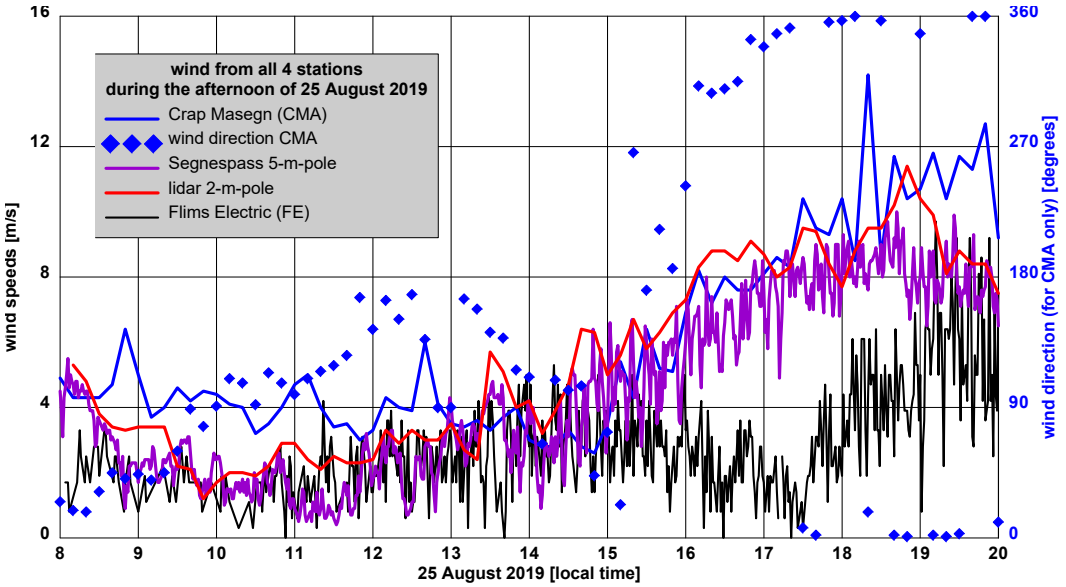

Figure 33: The average wind speeds of all the four stations discussed in this section (see figure 30). The 25 August 2019 was the day with the closest similarity to 4 August 2018. The gusts are not shown here in order to keep the graphics simple. They reached about 50 % above the 10-minute averages on both days (4 August 2018 and 25 August 2019).

Within the observations in summer 2019, 25 August 2019 was selected to have the closest similarity to 4 August 2018. This day allowed a direct comparison between the two operational stations and the two stations closer to the site of the accident operated in 2019 only. Figure 33 demonstrates that the wind at the Segnes pass closely followed the wind at Crap Masegn (CMA). This is a strong indication that the wind at Crap Masegn is representative of the wind across the Segnes pass for the day of the accident.

The FE station at the southern edge of the high plateau recorded about half of the wind speed observed at Crap Masegn during both days. This shows that the lower station is not fully exposed to the stronger downslope wind higher up in the valley. It decreases even more after 17:00 LT. The FE station would have been more important had the winds at the Segnes pass and at Crap Masegn not correlated so well. Then the wind at the Segnes pass could be estimated by doubling the speed measured at the FE station.

A1.7.15 Fine-scale wind field modelling using PALM

The regional COSMO-1 model of MeteoSwiss was introduced in section A1.7.12. This model, with a horizontal grid resolution of about 1 km, is able to analyse and predict the weather on a scale larger than a few kilometres. This is sufficient for depicting the general flow across the mountain range (figure 19). However, for simulating the turbulent flow within the basin south of the Segnes pass, it is necessary to have a much better resolution.

PALM[36] is a Large Eddy Simulation model (LES) allowing a chosen grid resolution of 10 m in order to simulate eddies with a diameter of 50 m or more. The LES is comparable to a CFD[37] model used in aerodynamics. PALM was adapted to the region around the Segnes pass at the Centre for Aviation at the Zurich University of Applied Sciences (ZHAW[38]). The model incorporates the topography of the terrain at this high resolution as well as other surface properties like soil moisture and albedo. The goal was to simulate the three-dimensional wind field, which is only partly known from the descriptions by eyewitnesses at the time of the accident (section A1.7.7).

The flow and the thermodynamic properties on the larger scale were taken from COSMO-1. Within PALM, three nested grids with horizontal spacings of 160, 40 and 10 m were introduced in three domains. In the following, only the inner domain (child domain) centred south-west of Piz Segnas is shown (figure 34).

At the beginning of the simulations, a sensitivity study assessed the influence of slightly different boundary conditions than offered by COSMO-1 (three wind directions and two stability classes). This study confirmed that the resulting flow patterns are quite robust. However, the best correlation with the observed winds was achieved by using the unchanged boundary conditions, including the neutral temperature profile.

[36] PALM: Parallelized large-eddy simulation model, https://palm.muk.uni-hannover.de/trac

[37] CFD: Computational fluid dynamics, with applications in aerodynamics and other disciplines in engineering

[38] https://www.zhaw.ch/en/engineering/institutes-centres/zav/

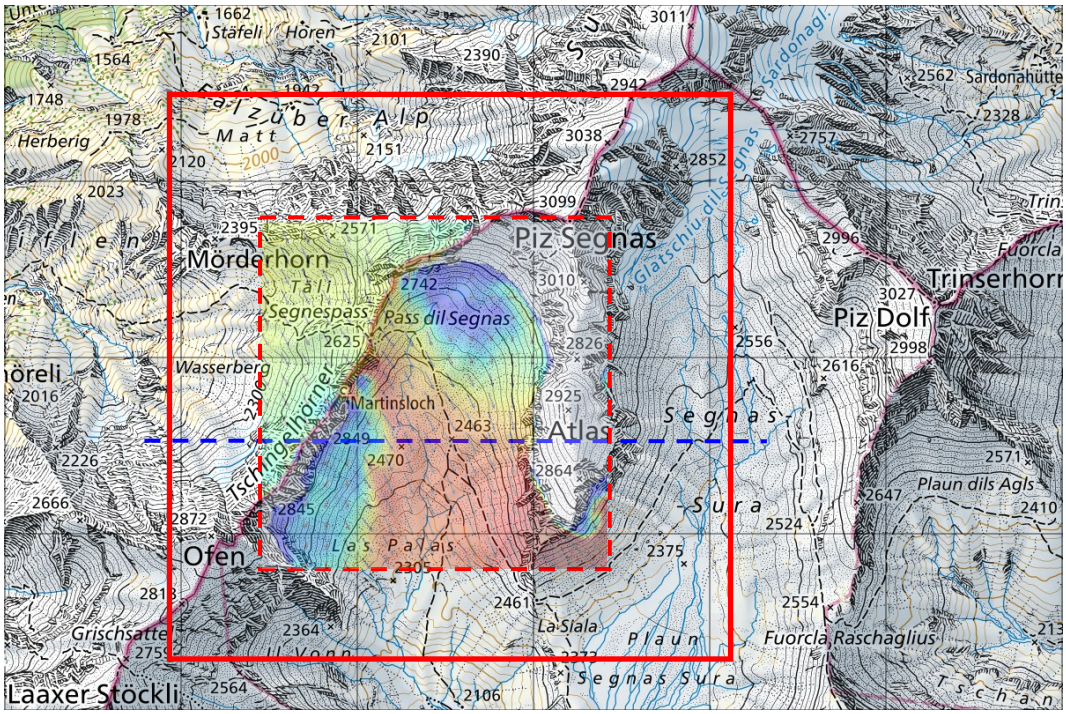

Figure 34: The square drawn with the solid red line is the inner domain (child domain) of PALM where the simulation was performed at the full resolution. The smaller square with the dashed boundary and a size of 2 km defines the area where the results are shown in figure 35. These are added here as a faint overlay for ease of orientation. The blue dashed horizontal line marks the position of the cross-sections shown in figure 36. Source of the map: Federal Office of Topography (swisstopo).

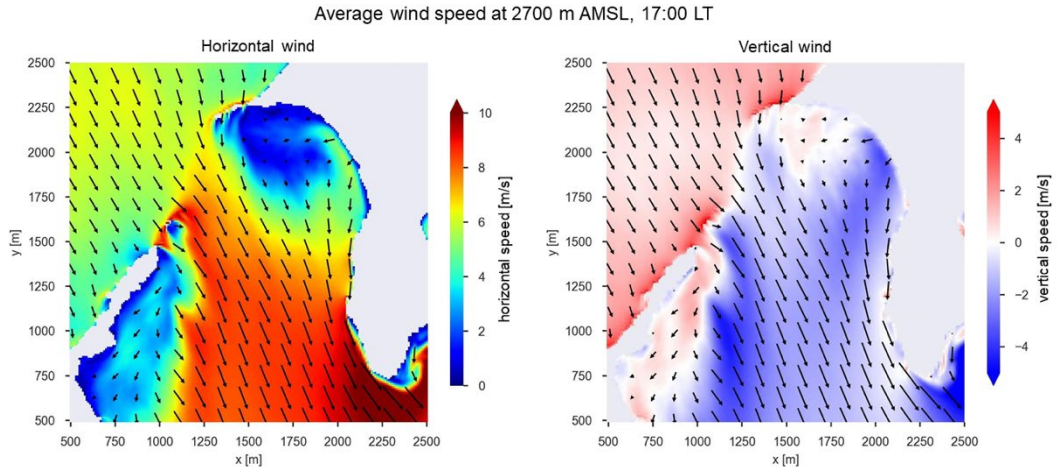

Figure 35: The horizontal wind field (left) and the vertical wind component (right) at 2,700 m AMSL as simulated by PALM (averages between 16:30 and 17:00 LT). The arrows depict the horizontal wind on both frames, but the colour coding is for horizontal wind speed on the left and vertical wind speed on the right. See further information below.

The main results for the three-dimensional wind field on 4 August 2018, around 17:00 LT, can be summarised by observing figures 35 and 36. It is important to note – even when the results are highly plausible – that this is not exactly the wind field encountered by HB-HOT. Therefore, the reconstructed flight track is not integrated in the graphs. This simulation shows – in combination with the measurements presented in section A1.7.14 – the general structure of the flow, with the ranges of values for wind speeds and turbulence both in the horizontal and vertical.

Since these are 30-minute averages, the position and strength of the main elements such as up- and downdraughts can vary. However, these averaged wind fields show tendencies, i.e. locations where lifting or sinking flows dominated.

The illustrations demonstrate that a rotor flow with considerable downdraught most likely developed on the downwind side (lee) of the western crest, whereas at the northern slope of the basin, updraughts dominated. The horizontal wind along the centre of the valley was enhanced (8 m/s or 16 kt), with maxima over the Segnes pass and at the southern edge of Atlas. A zone with much less wind is associated with the zone in the north, where thermal lift was active. Therefore – even when not projecting any details onto the reconstructed flight track – the following scenario is plausible. Initially, when entering the basin from the south, nose-wind and sinking were dominant. When approaching the Segnes pass, the zone with less wind and some thermal lift was encountered.

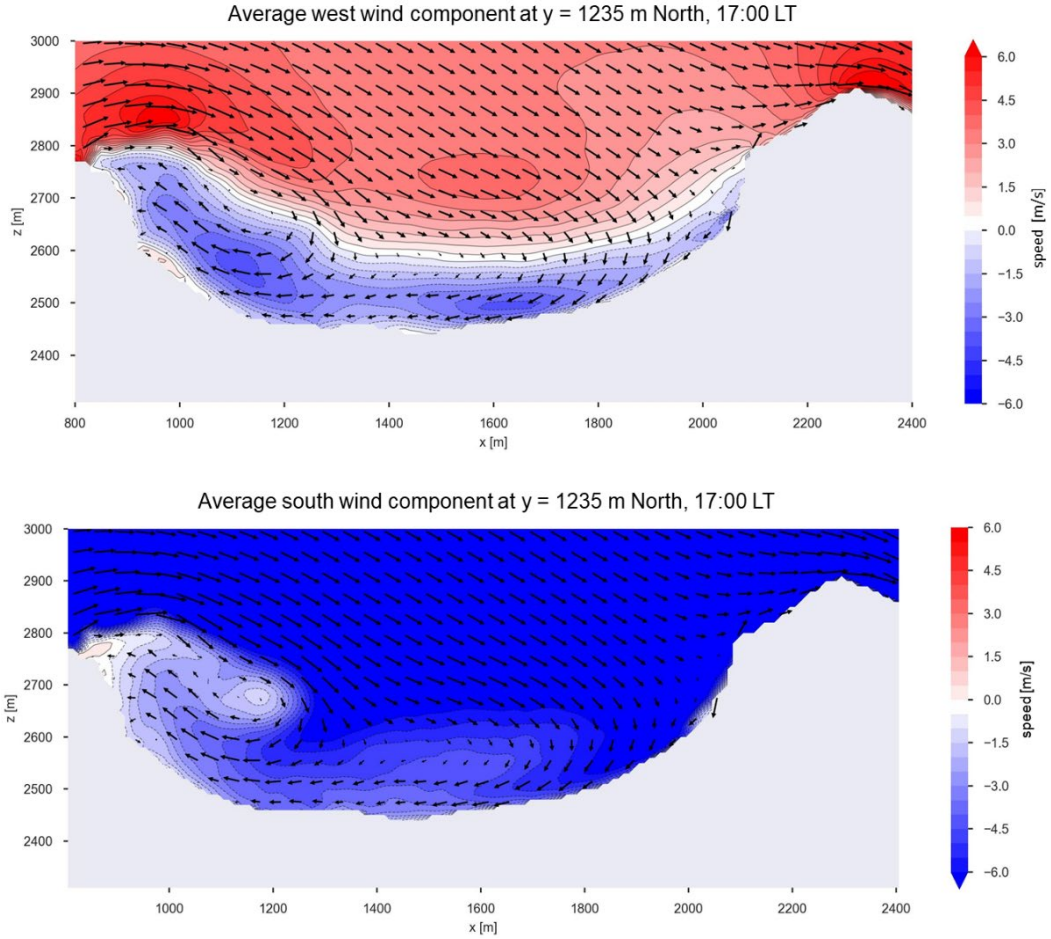

Figure 36: Vertical cross-section from west to east along the blue dashed line in figure 34. The arrows depict the flow on this plane in both frames, clearly showing the rotor behind the western crest (the Tschingelhörner range of mountain peaks on the map). The colours according to the scales on the right-hand side show the wind from the west (negative values from the east) in the upper frame, and the wind component from the north by the negative values in the lower frame. The wind components above the crest were about 7 m/s from the west and 8 m/s (outside of the colour scale) from the north, i.e. a north-westerly wind of about 21 kt above the basin. Near the western slope of Atlas in the east, the wind near the surface was from the north-east.

The two wind components near the surface in figure 36 are both about 5 m/s, resulting in roughly 15 kt from the north-east. This correlates with the wind observed[39] after the impact (17 kt from 060 to 070°), and is also in accordance with the descriptions of the eyewitnesses 15 minutes after the accident in section A1.7.7. The estimate of 60 km/h for the very local flow across the Segnes pass is plausible as well and is in the same order of magnitude as the maxima measured in 2019. The wind field shown in figure 35 is 75 m above the pass. For such comparisons, it is important to note that the results shown here are average wind speeds, whereas the observations are representative for shorter periods.

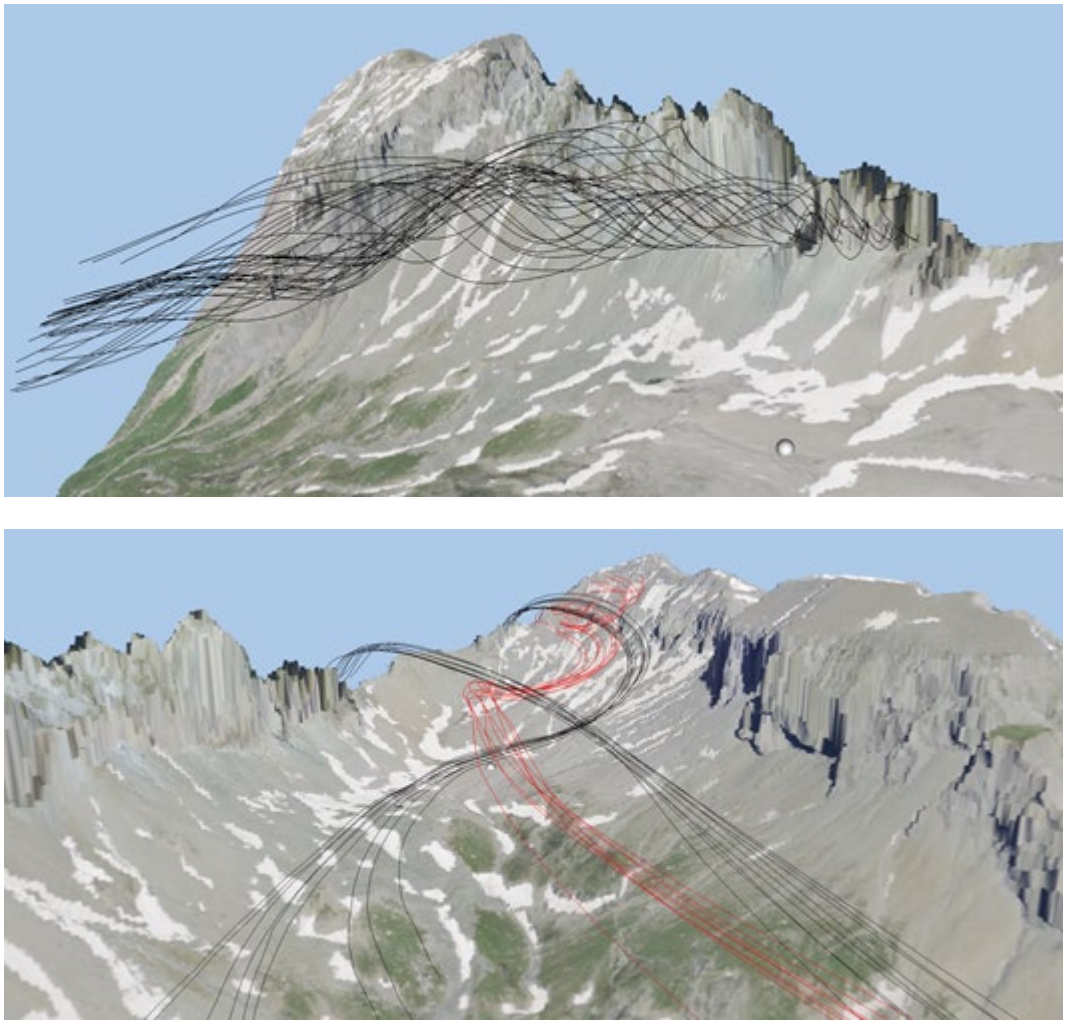

Figure 37: Three-dimensional display of selected streamlines in the region of the last minute of the flight. The site of the accident is marked by the white spheres. Top frame: Turbulent flow in the core of a rotor behind the western crest (the Tschingelhörner peaks on the map) seen from the east. Bottom frame: More laminar stratified flow near the surface. The lowest streamlines pass the site of the accident at a height of 10 m; the red ones at 100 m, and the higher black ones at 200 m. The north-easterly flow along the slope of Atlas and the north-westerly flow aloft are clearly visible. As emphasised above, this is a plausible flow pattern that can vary in time and space and must not be projected in detail to the reconstructed flight track.

[39] The wind was calculated by analysing the displacement of the dust cloud after the impact of HB-HOT to the ground.

PALM was also applied to five selected days from the summer of 2019, where continuous measurements on the Segnes pass and from the lidar station lower in the basin were available (see section A1.7.14). They compared well with one exception and therefore verified the reliability of the model adapted to this region.

This study shows that vertical wind speeds, as measured in the summer of 2019, were not exceptional and could therefore have been encountered at the time of the accident.

A1.7.16 Assessing some meteorological aspects

A1.7.16.1 Comparison of the actual weather conditions with the official forecast

The aviation weather forecasts – available on the morning and just before the flight (see section A1.7.5) – did not show any extraordinary or especially difficult conditions along the planned flight. The weather encountered during the flight was in accordance with the forecasts.

The forecast advised to be vigilant for possible showers or thunderstorms along the route. Considering the experience of the flight crew and the general weather conditions, it was clear that isolated showers or thunderstorms could have been avoided based on decisions during the flight. There was no risk that all VFR routes between Locarno and Dübendorf were closed. An alternative route along the Rhine Valley via Chur would have been possible if the Alpine ridge was in clouds. The crew was not forced to continue the flight across the Segnes pass. Even a return to Locarno or Lugano was possible at any time if the weather in the north deteriorated.

The convective activity with showers and a likelihood of thunderstorms was more pronounced than the previous day and was most likely to be observed visually.

A1.7.16.2 Turbulence during the last phase of the flight

The wind across the Segnes pass and over the basin south of it usually blows from the north-west during sunny afternoons (see sections A1.7.13 and A1.7.14.1). Enhanced afternoon wind speeds are also common in other Alpine passes.

Even more widely known, is the fact that downwind (in the lee) of ridges, turbulence should be expected. Additionally, at this time of the day, thermal activity with vertical wind speeds of ±3 m/s are normal. Dedicated measurements of the vertical wind (see section A1.7.14.2) show that even ±4 m/s are frequent, and extreme downdraughts up to -6 m/s are possible. The risk of encountering a sequence of rapidly changing vertical wind – which is a dangerous combination – cannot be excluded (see section A1.7.14.2). This risk for a change of 5 m/s or more within three or five seconds was quantified for 25 August 2019 to be one or two per cent, respectively. When flying 100 hours in comparable conditions, the exposition time to an enhanced risk is between one and two hours. This purely statistical view for a comparable day does not consider stationary shear zones like rotors or more wind as it was reported for 4 August 2018.

The wind at the time of the accident was stronger than a few hours earlier when the crew flew through the same region during their ferry flight from Dübendorf to Locarno in a single-engine aircraft. As recorded by the measuring station at Crap Masegn (see figure 32), the northerly wind had an increasing tendency. This increased wind at crest height most likely intensified the turbulence in the south-west of Piz Segnas.

The text forecast for general aviation (see section A1.7.5.1) indicated such a development of the upper-level wind, and the crew could have recognised it as a crosswind from the left while flying along the Rhine Valley and when entering the side valley south-west of Piz Segnas.

A1.7.16.3 Predictability of wind across Alpine passes

Thermal wind systems not only act on slopes and along valleys, but also lead to air mass exchange between different valleys, i.e. wind across passes. This is especially pronounced during summer, when the diurnal heating reaches higher altitudes (see section A1.7.13). It is possible to see these local winds in publicly-available weather prediction products. However, they are not part of a standard aviation weather briefing. Sometimes the pressure difference between Lugano and Zurich Airport is consulted as an indicator for a North- or South-Foehn events. However, this indicator is not specific for wind across Alpine valleys and can often lead to unexpected events.